ACS OMEGA

Open Access

http://pubs.acs.org/journal/acsodf

Article

Laccase-Catalyzed Biotransformation of Dihydrostilbenes and Phenanthrenes: A Route to Novel Natural Product Derivatives

Quentin Favre-Godal,* Laurence Marcourt, Manon Giraud, Zeinab Karmime, Rémy Marcellin-Gros, Lorène Gourguillon, Jean-Luc Wolfender, Katia Gindro,* and Emerson Ferreira Queiroz*

Cite This: https://doi.org/10.1021/acsomega.6c01880

Read Online

ACCESS | Metrics & More | Article Recommendations | Supporting Information

ABSTRACT: Biotransformation is an eco-friendly and effective strategy for enhancing the chemical diversity of natural products for biological screening. Among various biotransformation methods, laccase-mediated transformations have successfully yielded bioactive compounds across multiple chemical classes. In this study, laccases from *Trametes versicolor* were used to catalyze the biotransformation of the dihydrostilbene gigantol and the phenanthrenes flavidin and coleonin, leading to the formation of a series of structurally complex derivatives. The selected substrates were subjected to laccase-mediated biotransformation and the reactions were followed using state-of-the-art analytical techniques. Depending on the reaction conditions, the process led to the formation of multiple monomers, dimers and trimers. After optimization and scale-up of the biotransformation reactions, the crude mixtures were purified by high-resolution semipreparative HPLC using dry-load injection. This workflow enabled the isolation of 13 structurally diverse derivatives, with 10 compounds being reported for the first time. All products were comprehensively characterized using high-resolution mass spectrometry (HRMS) and nuclear magnetic resonance (NMR) spectroscopy. This study underscores the promising potential of fungal laccase-mediated biotransformation as a tool to diversify bioactive natural product structures, thereby generating novel scaffolds of interest for biological screening campaigns.

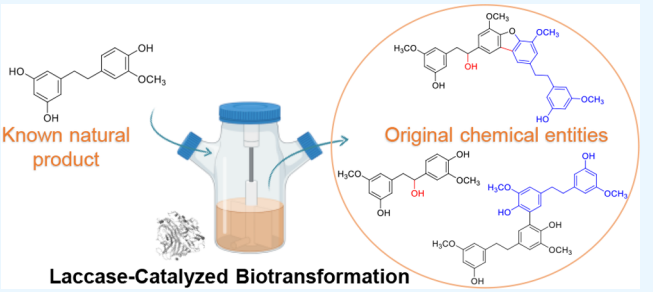

1. INTRODUCTION

The biotransformation reactions use whole organisms or isolated enzymes to catalyze structural modifications in organic compounds.[1−3] This approach has emerged as a promising and sustainable complementary tool, or alternative, to traditional chemical synthesis for diversifying natural products intended for biological screening.[1−3] Unlike conventional synthetic methods, which often require extensive use of organic solvents and frequently result in the generation of toxic byproducts[4] biotransformation offers significant advantages. Biotransformation processes typically operate under mild, aqueous conditions, reducing energy input and minimizing the formation of undesired byproducts as well as associated costs.[5] This enzymatic approach not only streamlines the modification process and enhances selectivity but also aligns with the principles of green chemistry, making it particularly valuable for cosmeceutical, pharmaceutical, and agrochemical research that seeks efficient and environmentally friendly routes to molecular diversification.

Recently, we demonstrated that biotransformation reactions can be effectively conducted utilizing a mixture of secreted enzymes, defined as the "secretome" of the saprophytic fungus *Botrytis cinerea*.[6] Using this strategy, several dimerized stilbene analogues were generated, with certain compounds displaying notable antifungal, antiviral, and antibacterial activities.[6−10] Most of the reactions observed using this approach were dimerization by coupling phenoxy radicals, most likely carried out by laccases secreted by the fungi.[10] In this context, the efficiency of the phenoxy radical coupling also depended on the substrate scaffold.[11]

Laccase-mediated biotransformation has emerged as a particularly promising strategy within isolated enzyme systems, demonstrating remarkable efficacy in generating bioactive compounds such as lignans, neolignans, dimeric stilbenoids, bioflavonoids, and biaryls.[6,10,12−14] Laccase is an enzyme belonging to the multicopper oxidase family. It can oxidize a wide range of substrates, particularly phenols and aromatic amines, by using molecular oxygen as an electron acceptor. Although laccases are predominantly studied in fungi, they have also been identified in bacteria, plants, and, to a lesser extent, in other organisms such as insects, algae, and some

Received: February 18, 2026
Revised: June 5, 2026
Accepted: June 15, 2026

marine invertebrates. In these systems, laccases or laccase-like enzymes participate in diverse physiological processes, including cuticle formation in insects and phenolic compound metabolism in algae and marine species.[12,15−17] In addition, laccases and laccase−mediator systems offer environmentally sustainable oxidation methods capable of substituting conventional chemical oxidants such as silver acetate for a broad range of substrates.[18,19] The use of toxic or hazardous catalysts in chemical oxidation poses substantial risks in handling and waste management, further emphasizing the advantages of greener enzymatic alternatives. Consequently, laccases represent highly attractive biocatalysts for selective oxidation and biotransformation processes.[2]

Among fungal sources, *Trametes versicolor* (L.) Lloyd, a white-rot fungus, is a well-known producer of laccases, playing a crucial role in lignin degradation and wood decomposition as part of its ecological function. During wood decomposition, these enzymes play a key role in the oxidative breakdown of lignin, allowing *T. versicolor* to access cellulose and other carbohydrates as sources of carbon and energy. In addition to lignin degradation, laccases contribute to the detoxification of phenolic compounds and play a role in the fungus's defense against microbial competitors. Due to its high redox potential, versatility of substrate, stability, and production yield, this enzyme is highly studied and used for biotechnological applications.[20,21]

Using known bioactive compounds as substrates for enzymatic modification provides a strategic advantage in molecular diversification. It facilitates the generation of novel analogs with potentially improved pharmacokinetic or pharmacodynamic profiles.[22] This approach also supports the systematic exploration of structure−activity relationships and expands chemical diversity in natural product-derived drug discovery.

Among the various classes of bioactive natural products, stilbenoids and phenanthrenoids represent particularly attractive candidates for enzymatic biotransformation. These two families are closely related at structural and biosynthetic levels, as phenanthrenoids are generally considered to arise from dihydrostilbenoid precursors through oxidative intramolecular cyclization reactions. Their structural diversity, combined with well-documented biological activities, has recently led to their use as starting points for the generation of complex compounds displaying a wide range of biological activities.[6,10,23−27] However, achieving the total synthesis of their oligomeric derivatives (dimers, trimers, and tetramers) through conventional organic chemistry remains highly challenging.[28−30] The intricate architectures, featuring multiple stereocenters, axial chirality, and fused ring systems, complicate regioselective coupling and protection strategies.[28−30] Oxidative oligomerization from monomers like resveratrol is difficult to control in terms of oligomer degree and stereochemistry, with increased steric hindrance yielding low product formation for higher oligomers.[28−30]

Stilbenoid compounds, derived from the shikimate pathway, are characterized by a structure consisting of two phenyl groups connected by an ethylene bridge.[31] Catalytic or enzymatic reduction of this central double bond yields dihydrostilbenes, a structurally related class of compounds. In plants, stilbenes are produced primarily as phytoalexins, protective secondary metabolites deployed in response to various environmental stresses, including pathogenic invasion and ultraviolet (UV) radiation.[32,33] The dihydrostilbene gigantol is commonly isolated from orchids. Gigantol exhibits antioxidant activity and cytotoxic activity against diverse cancer cell lines.[34,35] Interestingly, it inhibits the migratory behavior of nonsmall cell lung cancer cells. Gigantol has also been reported to inhibit the galactose-induced formation of cataracts by repressing the gene expression and activity of aldose reductase (AR) and inducible Nitric Oxide Synthase (iNOS).[36−39]

Phenanthrenoids are phenylpropanoid-derived specialized metabolites, characterized by a phenanthrene-type tricyclic aromatic core composed of three angularly fused benzene rings, variably substituted by phenolic, methoxy, glycosidic, or oxidized functionalities. Compounds with a saturated C-9-C-10 bond are classified as dihydrophenanthrenes. Other structural groups include phenanthrofurans, phenanthropyrans, and phenanthroquinones, with furan and pyran rings typically linked to the phenanthrene skeleton at the C-1-C-2 positions, though alternative linkages are also observed. The phenanthrenoids flavidin[40] and coelonin[41] are also metabolites found in orchid species from *Bletilla, Coelogyne, Pholidata, Bulbophyllum, Dendrobium*, and *Vanda* genera (LOTUS: Natural Products Online). Coelonin, has been described for its anti-inflammatory activities[42−47] and flavidin[40] showed antioxidant activity in various in vitro model systems.[40]

Stilbenoids and phenanthrenoids are of special interest for their roles in plant resistance to pathogens and their biological activities.[23,31,48] While the biotransformation of stilbenoids is relatively well described,[6,7,10,49] comparatively few studies have focused on dihydrostilbenes,[11,50] an even fewer on phenanthrenoids.[51,52] In this context, three biologically active metabolites, gigantol (dihydrostilbene), flavidin, and coelonin (phenanthrenoids) were therefore utilized as substrates in a laccase-catalyzed transformation system to evaluate their potential for generating structurally novel derivatives for further biological evaluation or modulation of the parent molecules.

2. RESULTS

To investigate the reactivity of the selected substrates under varying conditions, small-scale biotransformation experiments were carried out using 500 μg of substrate in a 0.5 mL reaction mixture and monitored by UHPLC-PDA-ELSD-MS (Supporting Information Figure S1). A range of organic solvent concentrations (10−70%) and laccase enzyme concentrations (10−100 U/mL of stock solution) was tested. Optimal conditions were defined by a marked decrease in the substrate signal and the appearance of multiple new peaks in the MS base peak intensity (BPI) chromatogram. Scale-up reactions were then performed with 20−50 mg of substrate in a 5−10 mL reaction mixture, monitored under the same UHPLC-PDA-ELSD-MS conditions. Once substrate consumption was complete, the reactions were stopped and the crude mixtures purified. The isolated derivatives were subsequently subjected to detailed spectroscopic analysis to enable unambiguous structural elucidation.

2.1. Biotransformation Reactions at the Analytical Scale

Among the multiple conditions evaluated for the biotransformation of gigantol (**1**), 30% of organic solvent, 30 μL of a laccase solution at 12.5 U/mL, and an incubation time of 9 h at room temperature generated many MS features, indicating the presence of hydroxyl (m/z 291 $[M + H]^+$), ethyl (m/z 319 $[M + H]^+$), and dimeric derivatives of gigantol (m/z 545−549 $[M + H]^+$) (Figure 1A). The appearance of major compounds **4**

https://doi.org/10.1021/acsomega.6c01880
ACS Omega XXXX, XXX, XXX−XXX

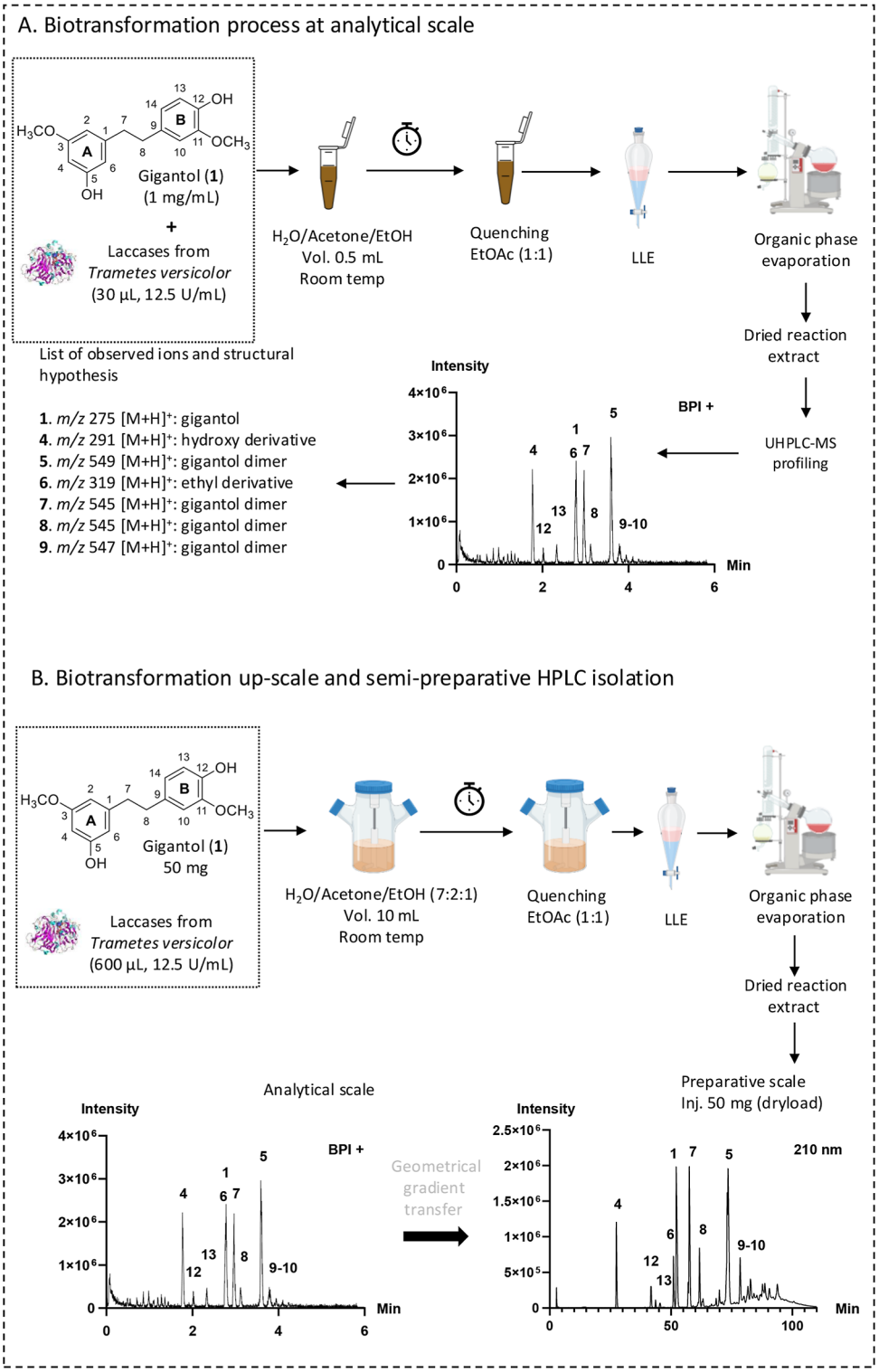

Figure 1. (A). Biotransformation process of gigantol (**1**) using laccases of *Trametes versicolor* at the analytical scale and UHPLC-MS profiling. (B). Upscaling of the biotransformation process of gigantol using laccases of *Trametes versicolor* and semipreparative HPLC-UV isolation of the generated compounds. Created with BioRender.com icons.

and **5**, often observed despite the numerous conditions tested, and other minor derivatives (**6**–**9**) suggested that gigantol was biotransformed, despite never being fully converted (Figure 2). However, when the incubation was shortened and a higher laccase concentration was used, additional unusual derivatives (**12** and **13**) were obtained, to the detriment of some minor derivatives previously detected (**7**, **11**) (Figure 2).

Among the conditions evaluated for flavidin (**2**) and coelonin (**3**), 40% of organic solvent, 30 μL of a laccase solution at 12.5 U/mL, and an incubation time of 3 h at room temperature generated new ion species (features) detected by mass spectrometry (MS) (**14**–**16**) and the total disappearance of the initial substrate (data not shown) (Figure 2).

https://doi.org/10.1021/acsomega.6c01880
ACS Omega XXXX, XXX, XXX−XXX

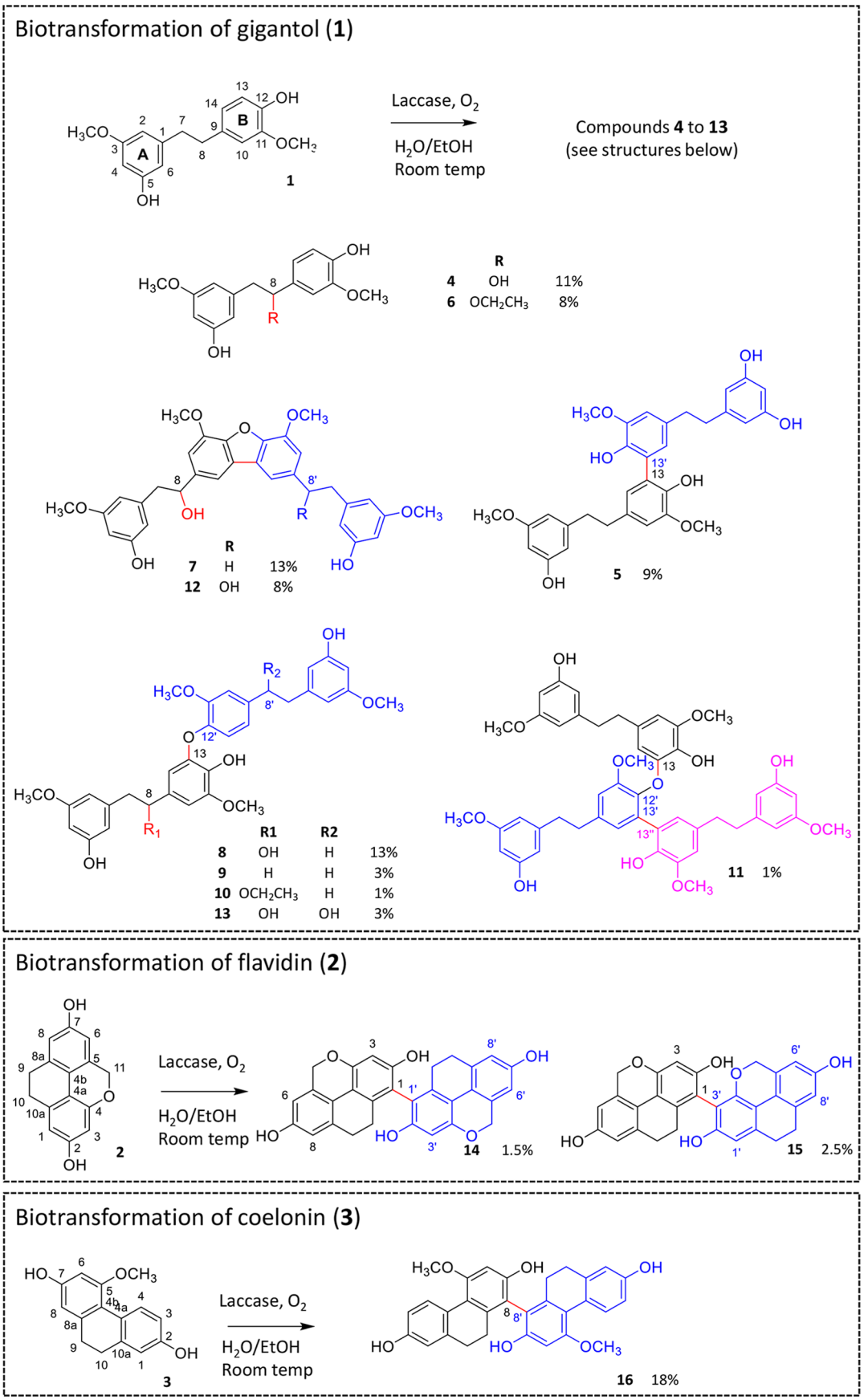

Figure 2. Isolated derivatives obtained from the biotransformation of gigantol (**1**), flavidin (**2**) and coelonin (**3**). The percentage indicated corresponds to the isolated product yield, calculated relative to the initial mass of the starting substrate.

https://doi.org/10.1021/acsomega.6c01880
ACS Omega XXXX, XXX, XXX−XXX

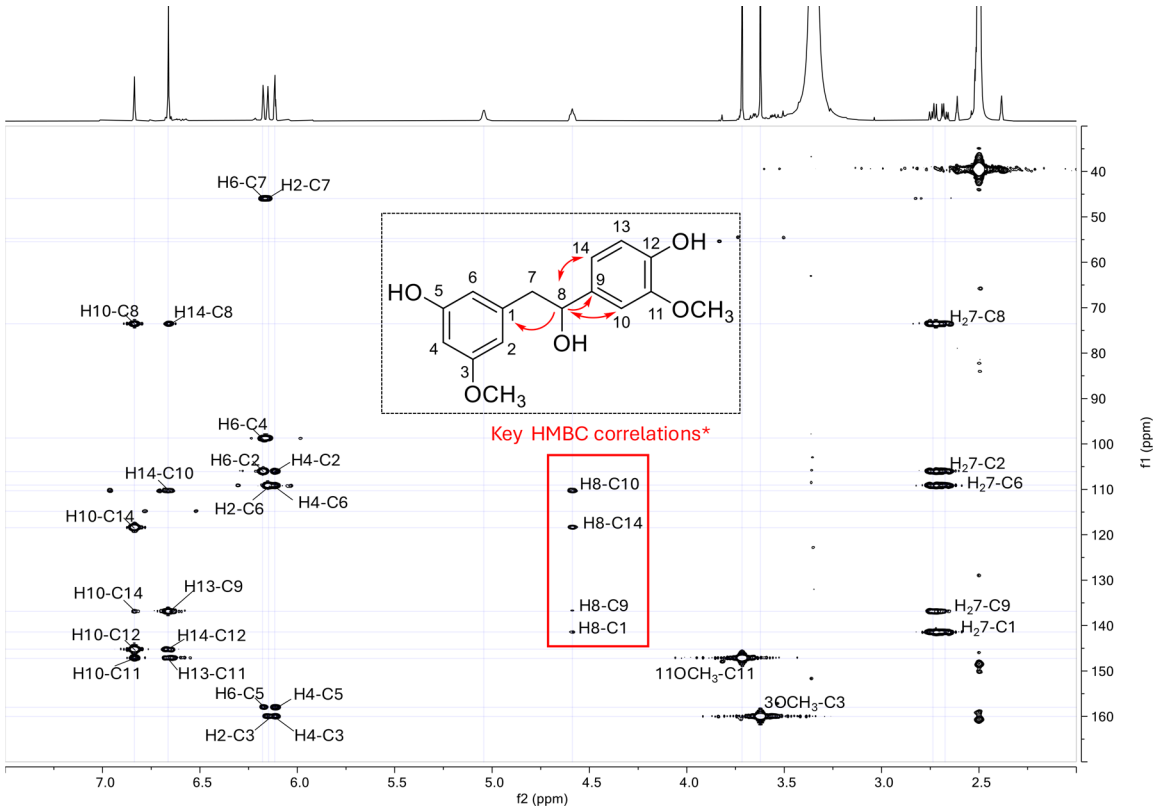

Figure 3. HMBC spectrum showing all the correlations observed for compound **3**.

A comparison of the MS traces before and after the reaction shows several peaks with molecular masses suggesting the presence of dihydrostilbenes or dihydrophenanthrenes, dimers of the original compounds.

2.2. Up-Scale Biotransformation, Isolation, and Structure Elucidation of the Generated Compounds

Up-scale experiments presented a similar metabolite profile to those observed at analytical scale, allowing us to use similar conditions as previously optimized. The reactions described above were therefore scaled up to enable the isolation and identification of the resulting derivatives by high-resolution mass spectrometry (HRMS) and nuclear magnetic resonance (NMR) spectroscopy, allowing unambiguous assignment of the key peaks detected during monitoring (Figure 1B).

Biotransformations of gigantol (**1**), flavidin (**2**), and coelonin (**3**) were subsequently carried out at an increased scale under the optimized conditions described above (see "Experimental" section). Following monitoring of the crude reaction mixtures, chromatographic separation parameters were refined at the UHPLC level. These optimized conditions were then successfully translated to both analytical HPLC, for control purposes, and semipreparative HPLC using geometric gradient transfer (Figure 1B).[53] The stationary-phase chemistry of the columns used was the same between all instruments to maintain the same chromatographic selectivity. Sample injections were performed using a dry load method according to a protocol recently developed in our laboratory,[54] allowing us to preserve a better resolution compared to a classical loop injection (Figure 1B).

Purification of the resulting reaction mixtures led to the isolation of 13 compounds (**1**−**13**) fully identified by NMR and HRMS analysis. Compounds **4**−**13** from the reaction with gigantol (**1**) (Figure 2), (**14**) and (**15**) from the reaction with flavidin (**2**), and finally **16** from coleonin (**3**) (Figure 2). Among the compounds isolated, **9** was identified as 4,5′,5‴-Trihydroxy-3′,3″,3‴,5-tetramethoxybibenzyl-3,4″-ether isolated from the *Bletilla striata* (Orchidaceae).[55] Compound **14** was identified as 1−1′-biflavidin, a previously described 9,10-dihydrophenanthropyran dimer from *Otochilus porrectus* (Orchidaceae).[56] while compound **16** was identified as blestriarene A.[57] The remaining compounds represent novel structures described herein for the first time.

Structural elucidation was based on HRMS data and interpreting the modifications of the 1D and 2D NMR signals compared to those expected for the original substrates. For example, for gigantol, its two aromatic rings can be easily differentiated by the chemical shifts and the multiplicity of their protons. Those of cycle A are in the form of three distinct triplets with the same coupling constant (∼2 Hz), while those of cycle B are in the form of two doublets (one with J ∼2 Hz and one with J ∼8 Hz), and a doublet of doublets (J ∼8, 2 Hz).

Compound **4** was isolated as a white amorphous solid. The specific rotation $[\alpha]_{20}D$ was near zero. The UV spectrum displayed absorption maxima at 225 and 276 nm. Compound **4** was assigned a molecular formula of $C_{16}H_{18}O_5$ according to the ESI$^-$-HRMS peak at m/z 289.1079 $[M - H]^-$ (calcd. $C_{16}H_{17}O_5$ for 289.1076) and 273.1119 $[M\text{-}H_2O + H]^+$ (calcd. $C_{16}H_{17}O_4$ for 273.1121). This corresponds to 16 uma more than gigantol (M = 274), corresponding to hydroxylation. The ^{1}H and HSQC spectra showed the presence of six aromatic protons and two methoxy groups, indicating that the two aromatic rings were conserved. In contrast, only one methylene was observed at δ_H 2.67 (1H, dd, J = 13.4, 5.6 Hz, H-7″) and 2.74 (1H, dd, J = 13.4, 7.7 Hz, H-7′) and one methine at δ_H 4.59 (1H, dd, J = 7.7, 5.6 Hz, H-8). These data and the

https://doi.org/10.1021/acsomega.6c01880
ACS Omega XXXX, XXX, XXX−XXX

presence of a hydroxyl at δ_H 5.04 (1H, br s, 8-OH) confirmed the hydroxylation of gigantol. The HMBC correlations of the methine with the carbons CH-10 (δ_C 110.3) and CH-14 (δ_C 118.5) position the hydroxyl in C-8, next to the B ring (Figure 3). Compound **4** was thus identified as 8-hydroxygigantol. To our knowledge, compound **4** is a new compound described here for the first time.

Compound **6** was isolated as a white amorphous solid. The specific rotation $[\alpha]_{20}D$ was near zero. The UV spectrum displayed absorption maxima at 229 and 280 nm. Compound **6** was assigned a molecular formula of $C_{18}H_{22}O_5$ according to the ESI$^-$-HRMS peak at m/z 317.1393 $[M - H]^-$ (calcd. $C_{18}H_{21}O_5$ for 317.1383). An ethyl group, probably coming from the ethanol in the reaction medium, is additionally observed at δ_H 1.03 (3H, t, J = 7.0 Hz) for the methyl, and 3.21 and 3.24 for the methylene, compared to those of compound **4**. As for compound **4**, the methine proton at δ_H 4.32 (1H, dd, J = 7.6, 5.8 Hz, H-8) showed a COSY correlation with the methylene protons H_2-7 (δ_H 2.66 and 2.87) and HMBC correlations with the CH-10 (δ_C 110.6) and CH-14 (δ_C 119.2) carbons of the B ring. Moreover, the HMBC cross-peak between H-8 and the methylene group of the ethyl substituent established the attachment of this side chain at C-8. Compound **6** was identified as 8-*O*-ethylgigantol, a new compound to our knowledge.

Compound **5** was isolated as a white amorphous solid. The UV spectrum displayed absorption maxima at 230 and 284 nm. Compound **5** was assigned a molecular formula of $C_{32}H_{34}O_8$ according to the ESI$^+$-HRMS peak at m/z 547.2315 $[M + H]^+$ (calcd. $C_{32}H_{35}O_8$ for 547.2326). The mass of **5** corresponds to a gigantol dimer, and signals corresponding to only one monomer are observed on the ^{1}H NMR spectrum, indicating a cyclization with an axis of symmetry. The aromatic proton H-13 of B ring is no longer observed, and H-10 and H-14 are observed as two doublets (J = 2.1 Hz) at δ_H 6.77 and 6.53, respectively; the cyclization is therefore made at C-13 for the two gigantol entities. To the best of our knowledge, compound **5** is a new compound and was named 13−13′-bigigantol.

Compound **7** was isolated as a white amorphous solid. The UV spectrum displayed absorption maxima at 228 and 284 nm. Compound **7** was assigned a molecular formula of $C_{32}H_{32}O_8$ according to the ESI$^+$-HRMS peak at m/z 545.2161 $[M + H]^+$ (calcd. $C_{32}H_{33}O_8$ for 545.2169) indicating a dimer of gigantol. Aromatics protons from two different ring A are identified at δ_H 6.11 (1H, t, J = 2.2 Hz, H-4), 6.20 (1H, t, J = 2.2 Hz, H-2), and 6.22 (1H, t, J = 2.2 Hz, H-6) for the first one and 6.13 (1H, t, J = 2.2 Hz, H-4′), 6.26 (1H, t, J = 2.2 Hz, H-6′), and 6.28 (1H, t, J = 2.2 Hz, H-2′) for the second one. The two B aromatic rings each consist of only 2 protons at δ_H 6.70 (1H, d, J = 2.0 Hz, H-14) and 6.65 (1H, d, J = 2.0 Hz, H-10) for the first one and 6.60 (1H, d, J = 2.0 Hz, H-14′), and 6.51 (1H, br s, H-10′) for the second one suggesting a dimerization between these two B rings. The HMBC correlations from H-10′ and H-14′ to the methylene CH_2-8′ at δ_C 37.2 and from H-10 and H-14 to the methine CH-8 at δ_C 74.3 indicate that, first, dimerization takes place between C-13 and C-13′ and, second, hydroxylation occurs at C-8. To match the molecular weight and formula, a 12-*O*-12′ cyclization is postulated. This is consistent with the fact that only 2 phenols from ring A are observed at δ_H 9.15 (1H, s, 5-OH) and 9.23 (1H, s, 5′-OH). To the best of our knowledge, **7** is a new compound and was named 8-hydroxy-12-*O*-12′,13−13′-bigigantol.

Compound **12** was isolated as a white amorphous solid. The UV spectrum displayed absorption maxima at 230 and 284 nm. Compound **12** was assigned a molecular formula of $C_{32}H_{32}O_9$ according to the ESI$^+$-HRMS peak at m/z 561.2115 $[M + H]^+$ (calcd. $C_{32}H_{33}O_9$ for 561.2119). As with compound **5**, with which it shares a certain spectral similarity, the mass of **12** corresponds to a gigantol dimer, while the observed NMR signals count as a monomer. The presence of an hydroxyl at C-8 (C-8′) was deduced from the HMBC correlation of H-10 and H-14 (H-10′ and H-14′) with C-8 (C-8′) and δ_C 73.8. The presence of only two protons for H-10 and H-14 (H-10′ and H-14′) at δ_H 6.82 and 6.66 for ring B indicated a 13−13′ cyclization. For the same reasons as compound **7** a 12-*O*-12′ cyclization is also postulated. As some signals are split, the presence of C-8/C-8′ isomers is also likely. To the best of our knowledge, **12** is a new compound and was named 8,8′-dihydroxy-12-*O*-12′,13−13′-bigigantol.

Compound **8** was isolated as a white amorphous solid. The UV spectrum displayed absorption maxima at 230 and 280 nm. Compound **8** was assigned a molecular formula of $C_{32}H_{34}O_9$ according to the ESI$^-$-HRMS peak at m/z 561.2125 $[M - H]^-$ (calcd. $C_{32}H_{33}O_9$ for 561.2119), which could also correspond to a gigantol dimer. The NMR spectra of **8** show close similarities to those of **7**, except that one of the two B rings retains its three aromatic protons at δ_H 6.49 (1H, d, J = 8.1 Hz, H-13′), 6.69 (1H, dd, J = 8.1, 1.9 Hz, H-14′), and 6.94 (1H, d, J = 1.9 Hz, H-10′) and that in addition to the two phenolic protons from ring A at δ_H 9.17 (1H, s, 5-OH), 9.28 (1H, s, 5′-OH) a phenol is observed at δ_H 8.48 (1H, s, 12-OH). These indicate that the cyclization between the 2 gigantol units occurs differently. On the HMBC spectrum, the phenol at δ_H 8.48 shows correlations with a carbon at δ_C 148.5 (C-11), which is linked to the methoxyl at δ_H 3.76 (11-OCH_3) and to a carbon at δ_C 143.9 (C-13). This methoxyl is positionned on the B-ring, which has only two aromatic protons since one of the two protons (the one at δ_H 6.65 (1H, d, J = 1.9 Hz, H-10)) correlates in HMBC with C-11 and in ROESY with the methoxyl. These indicate that the phenol in C-12′ (from the other gigantol unit) reacted with C-13 in the form of radicals. The HMBC correlation from H-10 and H-14 (δ_H 6.26) to the methine CH-8 at δ_C 73.5 allows the hydroxyl to be positioned. To the best of our knowledge, **8** is a new compound and was 8-hydroxy-13-*O*-12′-bigigantol.

Compound **10** was assigned a molecular formula of $C_{34}H_{38}O_9$ according to the ESI$^+$-HRMS peak at m/z 608.2849 $[M + NH_4]^+$ (calcd. $C_{34}H_{42}O_9N$ for 608.2854). Compound **10** coeluted with **9** during the anterior experiment. Additional orthogonal separation in normal phase was needed to separate those compounds. The NMR data of **10** showed close similarities to those of **8**, except that an ethyl group is observed at δ_H 0.99 (3H, t, J = 7.0 Hz) for the methyl and 3.23 (1H, dq, J = 9.4, 7.0 Hz) and 3.19 (1H, dq, J = 9.4, 7.0 Hz) for the methylene. The HMBC correlations of H-8 at δ_H 4.26 (1H, dd, J = 7.4, 6.3 Hz) to CH-10 at δ_C 105.4, CH-14 at δ_C 109.5, and to the methylene of the ethyl at δ_C 63.1 confirmed the structure of **10**. To our knowledge, **10** is a new compound and was named 8-*O*-ethyl-13-*O*-12′-bigigantol.

Compound **13** was isolated as a white amorphous solid. The UV spectrum displayed absorption maxima at 230 and 280 nm. Compound **13** was assigned a molecular formula of $C_{32}H_{34}O_{10}$ according to the ESI$^-$-HRMS peak at m/z 577.2074 $[M - H]^-$ (calcd. $C_{32}H_{33}O_{10}$ for 577.2068), which could also correspond to a gigantol dimer. The NMR data indicated that **13** share the

https://doi.org/10.1021/acsomega.6c01880
ACS Omega XXXX, XXX, XXX−XXX

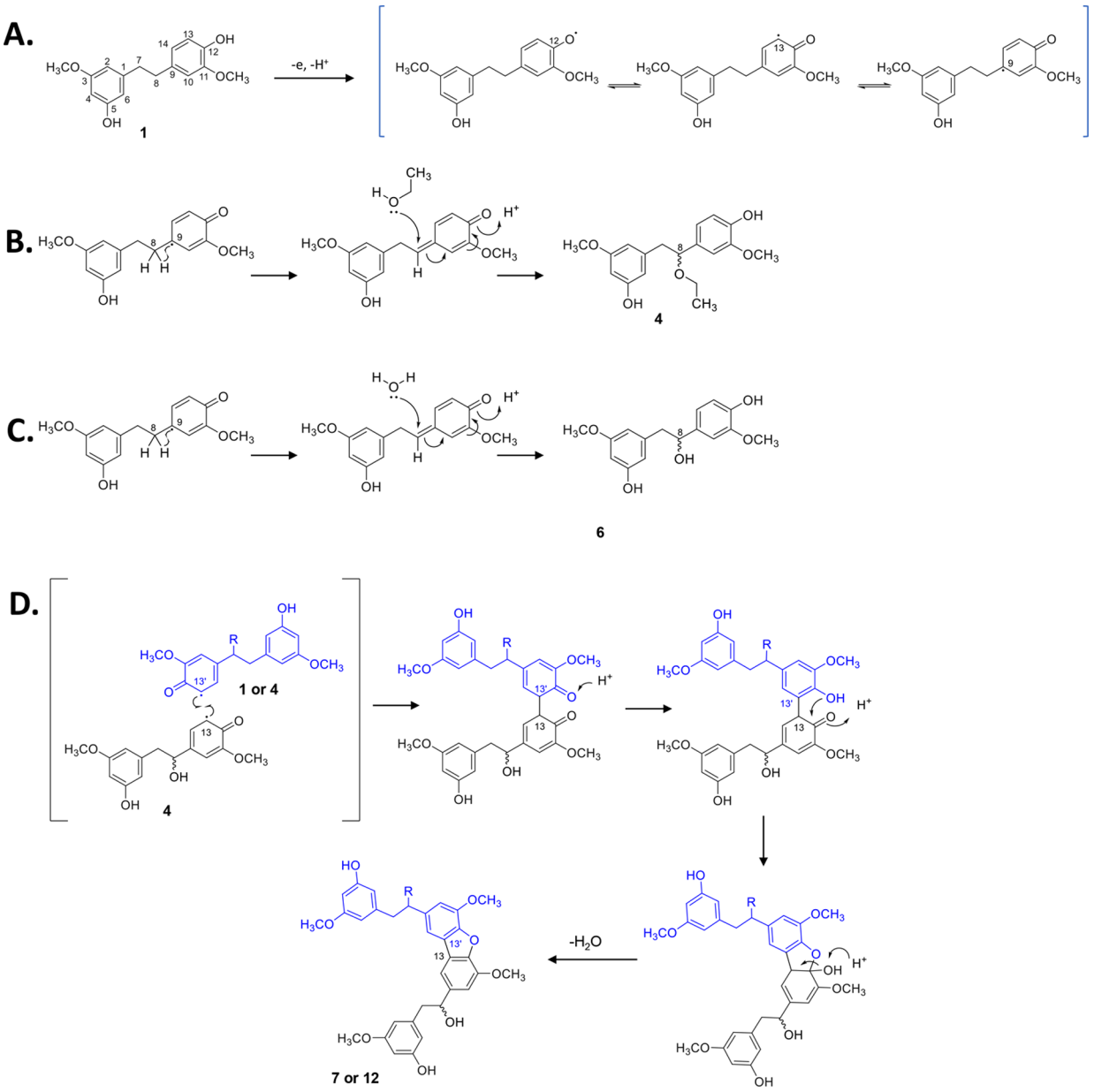

Figure 4. *T. versicolor* laccase-catalyzed radical formation on gigantol (**1**). Proposed mechanisms for the generation of compounds **4** (A) and **6** (B, C). Pathways to **7** and **12** (D).

same scaffold as **8**, **9** and **10**. As indicated by the HMBC correlations from H-10 (δ_H 6.65 and 6.66, d, J = 1.8 Hz) and H-14 (δ_H 6.27 and 6.28, d, J = 1.8 Hz) to C-8 at δ_C 73.4 and from H-10′ (δ_H 7.00, d, J = 1.9 Hz) and H-14′ (δ_H 6.77 and 6.78, dd, J = 8.2, 1.9 Hz) to C-8′ at δ_C 73.4, **13** was the dehydroxylated compound **9**. The splitting of some signals indicated that a mixture of C-8/C-8′ isomers probably occurred. To the best of our knowledge, **13** is a new compound and was named 8,8′-dihydroxy-13-*O*-12′-bigigantol.

Compound **11** was assigned a molecular formula of $C_{48}H_{50}O_{12}$ according to the ESI$^+$-HRMS peak at m/z 819.3357 $[M + H]^+$ (calcd. $C_{48}H_{51}O_{12}$ for 819.3375), which could correspond to a gigantol trimer. On the ^{1}H and COSY NMR spectra, the aromatic signals and their scalar correlations indicated that three A-ring are present and that three B-ring are all detected as 2 doublets at δ_H 5.95 (1H, d, J = 1.9 Hz, H-14), and 6.33 (1H, d, J = 1.9 Hz, H-10) for the first one, 6.79 (1H, d, J = 2.1 Hz, H-14′), and 6.95 (1H, d, J = 2.1 Hz, H-10′) for the second one and 6.59 (1H, d, J = 2.0 Hz, H-14″), and 6.68 (1H, d, J = 2.0 Hz, H-10″) for the third one. These indicated that they are all linked through their C-13. On the HMBC spectrum, H-10 and H-14 correlate with C-12 (δ_C 133.1), H-10, and the methoxy 11-OCH$_3$ with C-11 (δ_C 147.8), while H-14 correlates with C-13 at δ_C 146.7 showing that C-13 is linked to oxygen. For the second ring, H-10′ and H-14′ correlate with C-12′ (δ_C 138.7), H-10′ and the methoxy 11′-OCH$_3$ with C-11′ (δ_C 151.8), while H-14′ correlates with C-13′ at δ_C 124.4 showing that C-13′ is linked to a carbon. In the same way, H-10″ and H-14″ correlate with C-12″ (δ_C 141.6), H-10″ and the methoxy 11″-OCH$_3$ with C-11″ (δ_C 147.3) while H-14″ correlates with C-13″ at δ_C 132.9 showing that C-13″ is also linked to a carbon and therefore to C-13′. No oxygenated methine is observed in the ^{1}H and HSQC spectra, and six methylenes are detected at δc 36.9 (CH_2−8), 36.9 (CH_2-8″),

https://doi.org/10.1021/acsomega.6c01880
ACS Omega XXXX, XXX, XXX−XXX

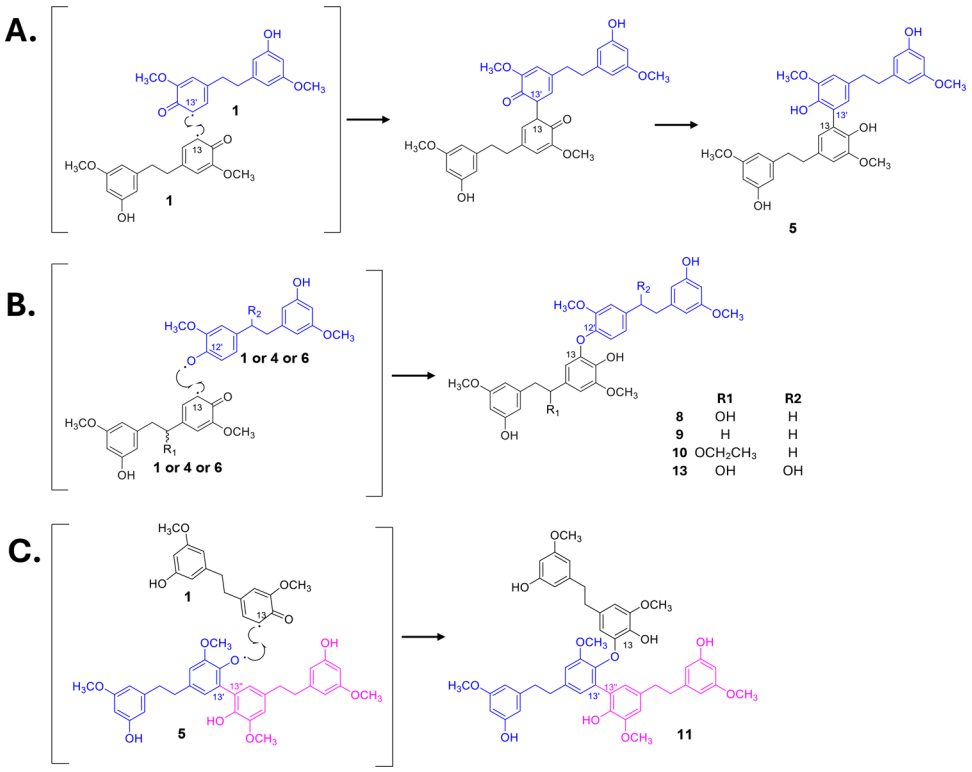

Figure 5. *T. versicolor* laccase-catalyzed radical formation on gigantol (**1**). Proposed mechanisms for the generation of compounds **5** (A), **8**−**10** and **13** (B), and **11** (C).

37.1 (CH_2-8′), 37.3 (CH_2-7′), 37.6 (CH_2-7″), and 37.8 (CH_2-7), confirming the trimer structure shown in Figure 2 for **11**. To our knowledge, compound **11** is new and was named 13-*O*-12′,13′-13″-trigigantol.

Finally, compound **15** was assigned a molecular formula of $C_{30}H_{22}O_6$ according to the ESI$^-$-HRMS peak at *m*/*z* 477.1332 [M-H]$^-$ (calcd. $C_{30}H_{21}O_6$ for 477.1333). The HRMS data of **15** indicated an isomer of **14**, and the NMR data showed that it was not a symmetrical dimer. The H-6 protons could be easily identified thanks to their HMBC correlations with the oxygenated methylene carbons CH_2-11: H-6 at δ_H 6.45 with CH_2-11 at δ_C 67.5 and H-6′ at δ_H 6.39 with CH_2-11′ at δ_C 67.3. The COSY correlations from H-6 to H-8 (δ_H 6.50) and from H-6′ to H-8′ (δ_H 6.55) indicate that dimerization did not occur at these cycles. Of the two remaining aromatic singlet, only one correlates in HMBC with a methylene carbon: H-1′ at δ_H 6.39 with CH_2-10′ at δ_C 27.3. The second singlet at δ_H 6.29, correlating with the aromatic carbons at δ_C 114.0 (C-1), 110.8 (C-4a), 151.5 (C-4), and 155.3 (C-2), was assigned to H-3. Compound **15** was thus identified as the C1−C3′ dimer of flavidin, a new compound named 1−3′-biflavidin.

3. DISCUSSION

Gigantol, flavidin, and coelonin were successfully biotransformed using purified *T. versicolor* laccase for the first time. This result is particularly noteworthy, as prior studies reported variable outcomes for stilbenoids lacking an exocyclic double bond[11,50] and required mediators (e.g., HBT or ABTS) for *T. versicolor* laccase-mediated phenanthrene degradation.[52] The ability of the laccase to catalyze these reactions under mild conditions, without mediator support, underscores its broad substrate specificity and potential for biocatalytic applications.[58] Among the tested substrates, flavidin and coelonin were more rapidly consumed than gigantol, suggesting faster reaction kinetics and inherent differences in substrate reactivity.

The inclusion of an organic solvent in the reaction medium, as previously reported in our work,[10] was essential to solubilize both the substrates and their transformation products. Noticeably, biotransformation occurred at organic solvent concentrations up to 70%; beyond this threshold, no detectable derivatives were observed at the analyzed time points. This observation highlights the laccase's notable tolerance to high organic content, which is an advantageous trait when balancing enzyme stability with the need to solubilize hydrophobic substrates and products.

Both incubation time and laccase concentration emerged as critical parameters influencing reaction outcomes. Specifically, high laccase concentrations or prolonged incubation led to the formation of visible precipitates, likely resulting from oxidative polymerization of phenolic intermediates.[6] This phenomenon was observed in parallel with a reduction in the number of newly detected ion species as observed in UHPLC-MS analyses and the appearance of a broad, unresolved hump in the UV baseline of the chromatogram, indicating high-molecular-weight, heterogeneous products.[59] A reciprocal relationship between enzyme concentration and incubation time was also evident: lower laccase levels necessitated extended incubation to achieve comparable degrees of substrate conversion.

The compounds produced through the various biotransformation reactions described below originate from phenoxy radical couplings catalyzed by laccases. These dimerization events preferentially occur on the *para*-hydroxyphenyl ring, in line with previously published findings on dihydroresveratrol.[11] The analysis of the yields of the isolated products indicates that

https://doi.org/10.1021/acsomega.6c01880
ACS Omega XXXX, XXX, XXX−XXX

derivatives in which the aromatic ring is directly connected via a regioselective biaryl C13′-C13 bond (**5**, **7**, **12**), thereby enabling hyper conjugative stabilization, are preferentially formed.[60] In contrast, dimers involving an oxygen atom as an intervening bridge are disfavored (compounds **9**, **10**, **13**), likely due to increased steric constraints and/or reduced electronic coupling, and therefore exhibit lower yields.[60]

Notably, based on literature precedents in laccase-mediated oxidation chemistry, compound **4** may plausibly arise from a nucleophilic water attack (solvolysis) at the sp^2-hybridized C-8 position of a para-quinone methide intermediate generated following oxidation of a *para*-hydroxyphenyl group (Figure 4). The isolation of compound **6** further supports the plausibility of this pathway, as its structure is consistent with a similar nucleophilic addition involving ethanol at the same reactive center. In this context, the role of the enzyme is proposed to involve the generation of the reactive quinone methide intermediate, whereas the subsequent trapping step likely depends on the reaction medium and solvent availability rather than direct enzymatic control. Accordingly, the incorporation of an ethoxy group in compound **6** is interpreted as resulting from solvent-mediated trapping of the intermediate by ethanol present in the reaction mixture. The near-zero optical rotation values observed for both compounds are also consistent with this hypothesis, suggesting the formation of racemic mixtures through a nonstereoselective process. Finally, the absence of analogous hydroxylated products in substrates lacking a para-hydroxy substituent further supports the proposed involvement of this functional group in enabling quinone methide formation and subsequent nucleophilic addition (data not shown). All these proposed reaction pathways warrant confirmation by computational mechanistic studies, which were not undertaken in the present work.

As for compound **4**, based on literature data, it can be hypothesized that the derivatives obtained from flavidin and coelonin, as the dimers obtained, resulted from phenoxy radical couplings. In all cases, the compounds dimerized in a favored position (**14**, **15**, and **16**), affording a hyper-conjugation between the aromatic rings (Figure 5).[60]

4. CONCLUSION

In this study, *T. versicolor* laccases efficiently catalyzed the oxidative coupling of gigantol, flavidin, and coelonin, affording 13 derivatives, 10 of which are new compounds reported here for the first time. Future biological evaluation of these derivatives, particularly antioxidant assays, given the known activities of the parent substrates, will be necessary to further assess their biological potential.

These findings underscore the enzyme's capacity for selective phenoxy radical dimerization, under mild conditions, without prior functionalization. Noticeably, oxidative coupling happened predominantly on the *para*-hydroxyphenyl ring, consistent with mechanisms previously observed in related stilbenoids.[6,10,11] Notably, compounds **4** and **6** appear to arise via nucleophilic attack (solvolysis) by water or ethanol on the sp^2-hybridized carbon at the C 8 position of a para quinone methide intermediate, itself generated by oxidation of a para hydroxyphenyl group. To the best of our knowledge, this represents the first report of such a derivative obtained from gigantol (or a closely related dihydrostilbene) under laccase-mediated conditions.

Overall, this work highlights fungal laccase-mediated biotransformation a a versatile and efficient approach for diversifying stilbenoid and phenanthrenoid scaffolds, generating structurally novel derivatives that constitute promising candidates for future biological screening campaigns.

5. MATERIALS AND METHODS

5.1. General Procedures

UV spectra were measured on a HACH UV−vis DR/4000 instrument (Loveland, CO, USA). NMR data were recorded on a Bruker Avance Neo 600 MHz NMR spectrometer equipped with a QCI 5 mm cryoprobe and a SampleJet automated sample changer (Bruker BioSpin, Rheinstetten, Germany). Chemical shifts are reported in parts per million (δ) using the residual DMSO-d_6 (δ_H 2.50; δ_C 39.5) as internal standards for ^{1}H and ^{13}C NMR, respectively, and coupling constants (J) are reported in Hz. Complete assignments were obtained based on 2D NMR experiments (COSY, ROESY, HSQC, and HMBC).

5.2. Materials

Gigantol (**1**) (CAS: 83088-28-2) was purchased from Extrasynthese, Lyon, France. Flavidin (**2**) (CAS: 83924-98-5) and coelonin (**3**) (CAS: 82344-82-9) and were purchased from ChemFaces, Hubei, People's Republic of China. Laccase from *T. versicolor* (CAS: 80498-15-3) was purchased from Merck, Darmstadt, Germany.

5.3. Biotransformation Reactions at the Analytical Scale Using a Laccase

The biotransformation reactions were carried out using pure compounds in 2 mL Eppendorf tubes. One compound was biotransformed at the time. The total volume of reactions was 0.5 mL. The final concentration of pure compounds (**1**, **2** or **3**) solubilized in EtOH was 1 mg/mL. The laccase was added last, with 30 μL of a solution at 12.5 U/mL in H_2O. The reaction was designed to have 10% EtOH, up to 60% acetone, and 30 to 90% H_2O (v/v). Once prepared, the mixtures were left in the dark, at room temperature, under constant gentle agitation. At the appropriate time (3−9 h), the reaction medium was extracted with 500 μL of ethyl acetate. The organic phase was dried under a nitrogen stream. Finally, the samples were solubilized in 200 μL of MeOH and analyzed by an ultrahigh performance liquid chromatography system equipped with a photodiode array, an evaporative light-scattering detector and a single quadrupole detector by heated electrospray ionization (UHPLC-PDA-ELSD-MS) (Waters, Milford, MA, United States).

5.4. UHPLC-PDA-ELSD-MS Analysis

UHPLC-PDA-ELSD-MS was used to compare the different extracts, control the purity of the fractions, and follow the biotransformation experiments. The chromatographic separations were done on an Acquity UPLC BEH C18 column (50 mm × 2.1 mm i.d., 1.7 mm; Waters, Milford, MA, USA), using a linear gradient from 5 to 100% B over 7 min, at a 600 μL/min flow rate. The solvent system consisted of [A]: H_2O with 0.1% formic acid and [B]: acetonitrile (ACN) with 0.1% formic acid. The injection volume was 2 μL, and the column was kept at 40 °C. ESI parameters were the following: capillary voltage 800 V, cone voltage 15 V, source temperature 120 °C, and probe temperature 600 °C. A full scan was acquired in negative and positive ionization modes with an m/z range of 150−1000 Da. The ELSD temperature was fixed at 45 °C, with a gain of 9. The PDA data were acquired from 190 to 500 nm, with a resolution of 1.2 nm. The sampling rate was set at 20 points/s. Data were processed using the MassLynx software (Waters, Milford, MA, United States).

5.5. Up-Scale Biotransformation and Isolation of New Derivatives

5.5.1. Up-Scale Biotransformation of Gigantol. For the upscale reaction with gigantol (50 mg), the total reaction volume was 10 mL, and the final concentration of gigantol was 5 mg/mL. The reaction was designed to have 10% EtOH, 20% acetone, and 70% H_2O (v/v). The laccase was added last, with 600 μL of a solution at 12.5 U/mL in H_2O. The reaction was stopped after 9 h with the

https://doi.org/10.1021/acsomega.6c01880
ACS Omega XXXX, XXX, XXX−XXX

Table 1. NMR Spectroscopic Data (600 MHz, DMSO-d_6) for Compounds 4 and 6

	compound 4		compound 6	
N°	δ_H (multiplicity,J)	δ_C	δ_H (multiplicity,J)	δ_C
1	-	141.4	-	140.9
2	6.15 (t, 2.2 Hz)	106.1	6.15 (d, 2.2 Hz)	105.8
3	-	160.0	-	159.9
4	6.11 (t, 2.2 Hz)	98.7	6.11 (t, 2.2 Hz)	98.9
5	-	158.0	-	158.0
6	6.18 (t, 2.2 Hz)	109.1	6.15 (d, 2.2 Hz)	109.0
7	2.74 (dd, 13.4,7.7 Hz) 2.67 (dd, 13.4,5.6 Hz)	46.0	2.87 (dd, 13.7,7.6 Hz) 2.66 (dd, 13.7,5.8 Hz)	44.0
8	4.59 (dd, 7.7,5.6 Hz)	73.5	4.32 (dd, 7.6,5.8 Hz)	81.8
9	-	136.9	-	133.1
10	6.84 (d, 1.4 Hz)	110.3	6.79 (d, 1.8 Hz)	110.6
11	-	147.2	-	147.4
12	-	145.2	-	145.7
13	6.66 (d, 1.4 Hz)	114.9	6.69 (d, 8.0 Hz)	115.0
14	6.66 (d, 1.4 Hz)	118.5	6.64 (dd, 8.0,1.8 Hz)	119.2
8-OCH_2CH$_3$			3.24 (dq, 9.5,7.0 Hz) 3.20 (dq, 9.5,7.0 Hz)	63.0
8-OCH$_2$$CH_3$			1.03 (t, 7.0 Hz)	15.3
3-OCH$_3$	3.62 (s)	54.7	3.62 (s)	54.7
11-OCH$_3$	3.72 (s)	55.5	3.72 (s)	55.5
5-OH	9.20 (s)	-	9.24 (s)	-
8-OH	5.04 (brs)	-	-	-
12-OH	8.74 (s)	-	8.87 (s)	-

addition of 10 mL of ethyl acetate. The organic phase was dried under a rotavapor.

The chromatographic separation of each crude dried reaction was performed on an XBridge C18 column (250 × 4.6 mm, i.d., 5 μm; Waters) equipped with a C18 precolumn at 1 mL/min, with [A]: H_2O and [B]: ACN both containing 0.1% formic acid as solvents. The UV absorbance was measured at 210 and 254 nm and the UV-PDA spectra were recorded between 190 and 600 nm (step 2 nm).

The geometrically transferred chromatographic gradients were applied at the semipreparative level using a Shimadzu HPLC system composed of LC-20A pump modules, an SPD-20A UV/vis detector, a 7725I Rheodyne injection valve, and an FRC-40 fraction collector (Shimadzu, Kyoto, Japan). Separations were carried out on an XBridge C18 column (250 × 19 mm, 5 μm; Waters) fitted with a C18 guard cartridge (10 × 19 mm, 5 μm; Waters). The mobile phase consisted of water ([A]) and acetonitrile ([B]), each supplemented with 0.1% formic acid, and was delivered at a flow rate of 15 mL/min. UV monitoring was performed at 254 and 280 nm. Samples were introduced using an in-house dry-load injection procedure.[61] The separation of the first gigantol reaction was pursued with 5% to 75% from 0 to 120 min. Fifteen fractions were obtained and were dried with the Genevac. F4 afforded compound **4** (5.5 mg, 11% of the substrate mass biotransformed). F7 afforded compound **6** (4 mg, 8%). F9 afforded compound **7** (6.5 mg, 13%). F10 afforded compound **8** (6.5 mg, 13%). F13 afforded compound **5** (4.5 mg, 9%). F15 afforded compound **11** (0.5 mg, 1%). Fraction F14 presented a mixture of compounds. This fraction was purified by normal phase chromatography using silica stationary phase. The sample (3 mg) was solubilized in EtOAc (HPLC grade) and purified using a HPLC 1100 system (Agilent series 1100) equipped with a normal phase Sunfire Prep Silica, 250 × 4.6 mm i.d., 5 μm). The solvent system consisted of [A]: hexane and [B]: EtOAc. The flow rate was set at 1 mL/min. The gradient was 30% of B to 80% of B in 60 min. The UV detection was set to 280 nm. Peaks were manually collected and corresponded to compounds **9** (1.5 mg, 3%) and **10** (0.5 mg, 1%).

A second reaction with gigantol (50 mg), was performed with 600 μL of a laccase solution at 12.5 U/mL in H_2O, and 40% acetone instead of the 10% previously. The reaction was stopped after 3 h by adding 10 mL of ethyl acetate. The organic phase was dried under rotavapor. The second reaction was separated following the same procedure. The separation was performed on an XBridge C18 column (250 × 19 mm i.d., 5 μm; Waters) equipped with a C18 precolumn cartridge holder (10 m × 19 mm i.d., 5 μm; Waters) at 15 mL/min, with [A]: H_2O and [B]: ACN both containing 0.1% formic acid as solvents. The UV detection was set at 254, and 280 nm. The mixtures were injected using a dry-load methodology developed in our laboratory.[61] F5 afforded compound **12** (4 mg, 8%) and F6 afforded compound **13** (1.5 mg, 3%).

5.5.2. Up-Scale Biotransformation of Flavidin or Coelonin. For flavidin (20 mg), or coelonin (20 mg) biotransformation reactions, the total reaction volume was 5 mL, and the final concentration of pure compound was 4 mg/mL. The reaction was designed to have 10% EtOH, 30% acetone, and 60% H_2O (v/v). The laccase was added last, with 30 μL of a solution at 12.5 U/mL in H_2O. The reactions were stopped after 9 h by adding 5 mL of ethyl acetate. The organic phase was dried under a nitrogen stream. The isolation of the flavidin biotransformation reaction was performed on C18 column (250 × 10 mm; 5 μm, OBD XBridge Prep C18) Waters and a C18 precolumn cartridge (10 × 10 mm i.d.). The separation was pursued with 5% to 75% B from 0 to 120 min. The flow rate was set at 4.5 mL/min. The fraction containing the significant products (2.1 mg) was dried and solubilized in EtOAc to be reinjected multiple times in the HPLC system in the normal phase (column Sunfire Prep Silica, 250 × 4.6 mm i.d., 5 μm). The isocratic condition was 40% of B during 30 min. Peaks detected at 280 nm were manually collected and corresponded to compounds **14** (0.3 mg, 1.5% of the substrate mass biotransformed), 8,8′-biflavidin, and **15** (0.5 mg, 2.5%). The biotransformed coelonin mixture was introduced similarly to the flavidin mixture. The separation was pursued with 8% to 85% B from 0 to 80 min. The flow rate was set at 4.5 mL/min. Major peaks detected at 280 nm were manually collected and corresponded to compound **16**, blestriarene A (3.6 mg, 18%).

5.6. UHPLC-dd-HRMS^2

The purified derivatives were characterized using an Acquity I-Class UPLC-PDA platform (Waters, Milford, MA, USA) hyphenated to a Q-Exactive Focus mass spectrometer (Thermo Scientific, Bremen, Germany) fitted with a heated electrospray ionization source (HESI-II). Chromatographic analyses were performed on a BEH C18 column (50 × 2.1 mm, 1.7 μm; Waters) employing a linear gradient from 5% to 100% solvent B over 7 min at a flow rate of 600 μL/min. The mobile phases consisted of water containing 0.1% formic acid

https://doi.org/10.1021/acsomega.6c01880
ACS Omega XXXX, XXX, XXX−XXX

Table 2. NMR Spectroscopic Data (600 MHz, DMSO-d_6) for Compound 5, 7 and 12[a]

	compound 5		compound 7		compound 12	
N°	δ_H (Multiplicity,J)	δ_C	δ_H (multiplicity,J)	δ_C	δ_H (multiplicity,J)	δ_C
1	-	144.0	-	142.0	-	141.7
2	6.27 (t, 2.0 Hz)	104.9	6.20 (t, 2.2 Hz)	106.0	6.21 (t, 1.8 Hz)	105.9
3	-	160.3	-	160.0	-	160.0
4	6.15 (t, 2.0 Hz)	98.8	6.11 (t, 2.2 Hz)	98.8	6.12 (t, 1.8 Hz)*	98.8
5	-	158.3	-	158.0	-	157.9
6	6.25 (t, 2.0 Hz)	108.1	6.22 (t, 2.2 Hz)	109.2	6.24 (t, 1.8 Hz)	109.2
7	2.72 (m)	37.8	2.78 (dd, 13.4,7.7 Hz) 2.69 (dd, 13.4,5.5 Hz)	46.1	2.72 (m)	46.1
8	2.73 (m)	36.8	4.57 (dd, 7.7,5.5 Hz)	74.3	4.61 (m)	73.8
9	-	131.4	-	no	-	134.8
10	6.77 (d, 2.1 Hz)	110.9	6.65 (d, 2.0 Hz)	108.4	6.82 (s)	108.4
11	-	147.7	-	149.7	-	147.9
12	-	142.1	-	147.3	-	144.5
13	-	126.1	-	128.6	-	126.4
14	6.53 (d, 2.1 Hz)	122.8	6.70 (d, 2.0 Hz)	120.5	6.66 (d, 2.0 Hz)#	120.5
5-OH	no	-	9.15 (s)	-	no	-
8-OH	no	-	4.83 (s)	-	5.01 (s)	-
3-OCH_3	3.66 (s)	54.8	3.62 (s)	54.7	3.63 (s)	54.8
11-OCH_3	3.78 (s)	55.8	3.68 (s)	55.6	3.76 (s)	55.8
1′	-	144.0	-	142.0	-	141.7
2′	6.27 (t, 2.0 Hz)	104.9	6.28 (t, 2.2 Hz)	104.9	6.21 (t, 1.8 Hz)	105.9
3′	-	160.3	-	160.3	-	160.0
4′	6.15 (t, 2.0 Hz)	98.8	6.13 (t, 2.2 Hz)	98.8	6.13 (t, 1.8 Hz)*	98.8
5′	-	158.3	-	158.3	-	157.9
6′	6.25 (t, 2.0 Hz)	108.1	6.26 (t, 2.2 Hz)	108.0	6.24 (t, 1.8 Hz)	109.2
7′	2.72 (m)	37.8	2.69 (s)	38.4	2.72 (m)	46.1
8′	2.73 (m)	36.8	2.69 (s)	37.2	4.61 (m)	73.8
9′	-	131.4	-	no	-	134.8
10′	6.77 (d, 2.1 Hz)	110.9	6.51 (brs)	110.7	6.82 (s)	108.4
11′	-	147.7	-	149.7	-	147.9
12′	-	142.1	-	147.3	-	144.5
13′	-	126.1	-	128.6	-	126.4
14′	6.53 (d, 2.1 Hz)	122.8	6.60 (d, 2.0 Hz)	122.2	6.68 (d, 2.0 Hz)#	120.5
5′-OH	no	-	9.23 (s)	-	no	-
8′-OH	no	-	-	-	5.01 (s)	-
3′-OCH_3	3.66 (s)	54.8	3.66 (s)	54.7	3.63 (s)	54.8
11′-OCH_3	3.78 (s)	55.8	3.67 (s)	55.6	3.76 (s)	55.8

[a]* and #: interchangeable values.

([A]) and acetonitrile containing 0.1% formic acid ([B]). The column temperature was maintained at 40 °C and 2 μL of sample were injected for each analysis.

Mass spectrometric acquisition was carried out in both positive and negative ionization modes. The HESI source settings were adjusted as follows: spray voltage +3.5 kV (−2.5 kV in negative mode), heater temperature 220 °C, capillary temperature 350 °C, S-lens RF level 45, sheath gas flow 55, and auxiliary gas flow 15 (arbitrary units). The setup was additionally connected to a Charged Aerosol Detector (Thermo Scientific, Bremen, Germany) operated at 40 °C. PDA data were recorded between 210 and 400 nm with a spectral resolution of 1.2 nm. Instrument operation and data acquisition were managed using Xcalibur 3.1 software (Thermo Scientific).

MS acquisition consisted of one full-scan event acquired at 35,000 fwhm resolution (m/z 200), followed by three data-dependent MS/MS scans (Top 3) recorded at 17,500 fwhm over an m/z range of 100−1500. The dd-MS2 events were acquired in discovery mode using Apex triggering (2−7 s), with a dynamic exclusion duration of 2 s, an isolation window of 1.5 Da, and stepped normalized collision energies of 15, 30, and 45. Additional acquisition settings included a default charge state of 1, an AGC target of 2.0×10^5, a maximum injection time of 119 ms, a loop count of 3, a minimum AGC target of 2.6×10^4, and an intensity threshold of 1.[62]

5.7. Description of the Isolated Compounds

8-hydroxygigantol (**4**): NMR data see Table 1. HRESIMS m/z 289.1079 $[M - H]^-$ (calcd. $C_{16}H_{17}O_5$ for 289.1076, Δ = 1.04 ppm).

13−13′-bigigantol (**5**): NMR data see Table 2. HRESIMS m/z 547.2315 $[M + H]^+$ (calcd. $C_{32}H_{35}O_8$ for 547.2326, Δ = −2.01 ppm).

8-*O*-ethylgigantol (**6**): NMR data see Table 1. HRESIMS m/z 317.1393 $[M-H]^-$ (calcd. $C_{18}H_{21}O_5$ for 317.1383, Δ = 3.15 ppm).

12-*O*-12′,13−13′-bigigantol (**7**): NMR data see Table 2. HRESIMS m/z 545.2161 $[M + H]^+$ (calcd. $C_{32}H_{33}O_8$ for 545.2169, Δ = −1.47 ppm).

8-hydroxy-13-*O*-12′-bigigantol (**8**): NMR data see Table 3. HRESIMS m/z 545.2161 $[M + H]^+$ (calcd. $C_{32}H_{33}O_8$ for 545.2169, Δ = −1.47 ppm).

4,5′,5‴-Trihydroxy-3′,3″,3‴,5-tetramethoxybibenzyl-3,4″-ether (**9**): NMR data see Table 3. HRESIMS m/z 547.2314 $[M + H]^+$ (calcd. $C_{32}H_{35}O_8$ for 547.2326, Δ = −2.19 ppm).

8-*O*-ethyl-13-*O*-12′-bigigantol (**10**): NMR data see Table 3. HRESIMS m/z 608.2849 $[M + NH_4]^+$ (calcd. $C_{34}H_{42}O_9N$ for 608.2854, Δ = −0.82 ppm).

13-*O*-12′,14′-13″-trigigantol (**11**): NMR data see Table 4. HRESIMS m/z 819.3357 $[M + H]^+$ (calcd. $C_{48}H_{51}O_{12}$ for 819.3375, Δ = −2.20 ppm).

https://doi.org/10.1021/acsomega.6c01880
ACS Omega XXXX, XXX, XXX−XXX

Table 3. NMR Spectroscopic Data (600 MHz, DMSO-d_6) for Compounds 8−10 and 13[a]

	compound 8		compound 9		compound 10		compound 13	
N°	δ_H (multiplicity,J)	δ_C	δ_H (multiplicity,J)	δ_C	δ_H (multiplicity,J)	δ_C	δ_H (Multiplicity,J)	δ_C
1		141.0	-	143.6	-	143.8	-	141.1
2	6.09 (t, 2.2 Hz)	105.9	6.18 (t, 2.2 Hz)	104.9	6.10 (t, 2.2 Hz)	105.8	6.11 (t, 1.9 Hz)	105.9
3	-	159.9	-	160.2	-	159.9	-	159.9
4	6.11 (t, 2.2 Hz)	98.8	6.12 (t, 2.2 Hz)	98.7	6.12 (t, 2.2 Hz)	98.9	6.12 (t, 1.9 Hz)	98.7
5	-	158.0	-	158.2	-	157.9	-	158.0
6	6.10 (t, 2.2 Hz)	109.2	6.16 (t, 2.2 Hz)	108.0	6.08 (t, 2.2 Hz)	109.0	6.10 (t, 1.9 Hz)	109.2
7	2.70 (dd, 13.3,7.3 Hz) 2.61 (dd, 13.3,6.0 Hz)	46.1	2.65 (m)	37.3	2.81 (dd, 13.0,7.4 Hz) 2.60 (dd, 13.0,6.3 Hz)	44.0	2.69 (dd, 12.9,7.1 Hz) ×2 2.62 (dd, 12.9,5.8 Hz) ×2	46.0
8	4.53 (q, 7.3 Hz)	73.5	2.65 (m)	36.5	4.26 (dd, 7.4,6.3 Hz)	81.7	4.53 (m)	73.4
8-O$CH_2$$CH_3$					3.23 (dq, 9.4,7.0 Hz) 3.19 (dq, 9.4,7.0 Hz)	63.1		
8-OCH$_2$$CH_3$					0.99 (t, 7.0 Hz)	15.2		
9		136.1	-	131.8	-	132.3	-	136.0
10	6.65 (d, 1.9 Hz)	105.2	6.60 (d, 1.9 Hz)	107.6	6.61 (d, 1.8 Hz)	105.4	6.65 (d, 1.8 Hz)/6.66 (d, 1.8 Hz)	105.2
11	-	148.5	-	148.7	-	148.7	-	148.6
12	-	136.1	-	135.5	-	136.3	-	136.2
13	-	143.9	-	144.0	-	144.1	-	143.8
14	6.26 (m)	109.2	6.18 (d, 1.9 Hz)	111.4	6.19 (d, 1.8 Hz)	109.5	6.27 (d, 1.8 Hz)/6.28 (d, 1.8 Hz)	109.2
3-OMe	3.61 (s)	54.7	3.63 (s)	54.8	3.61 (s)	54.7	3.61 (s)	54.8
5-OH	9.17 (s)	-	9.21 (s)	-	9.17 (s)	-	9.21 (s)	-
8-OH	5.10 (d, 4.5 Hz)	-	-	-			5.10 (d, 4.3 Hz)/5.11 (d, 4.3 Hz)	-
11-OMe	3.76 (s)	55.9	3.77 (s)	55.9	3.77 (s)	56.0	3.76 (s)	55.7
12-OH	8.48 (s)	-	8.42 (s)	-	8.58 (s)	-		
1′		143.8	-	143.8	-	140.5	-	141.4
2′	6.26 (m)	104.9	6.25 (t, 2.2 Hz)	104.9	6.26 (t, 2.2 Hz)	104.9	6.19 (t, 1.8 Hz)/6.18 (t.1.8 Hz)	106.0
3′	-	160.3	-	160.3	-	160.3	-	160.0
4′	6.15 (t, 2.2 Hz)	98.8	6.15 (t, 2.2 Hz)	98.8	6.15 (t, 2.2 Hz)	98.8	6.14 (t, 1.8 Hz) ×2	98.8
5′	-	158.4	-	158.3	-	158.3	-	158.0
6′	6.26 (m)	108.0	6.25 (t, 2.2 Hz)	108.0	6.25 (t, 2.2 Hz)	107.9	6.23 (t, 1.8 Hz) ×2	109.2
7′	2.74 (m)	37.4	2.74 (m)	37.4	2.74 (m)	37.4	2.75 (m)	45.9
8′	2.78	36.7	2.78 (m)	36.6	2.79 (m)	36.6	4.67 (m)	73.4
9′	-	136.8	-	136.8	-	137.0	-	141.2
10′	6.94 (d, 1.9 Hz)	113.3	6.93 (d, 2.0 Hz)	113.3	6.94 (d, 2.0 Hz)	113.2	7.00 (d, 1.9 Hz) ×2	110.8
11′	-	149.6	-	149.5	-	149.6	-	149.5
12′	-	144.0	-	144.1	-	143.7	-	144.7
13′	6.49 (d, 8.1 Hz)	117.6	6.53 (d, 8.1 Hz)	117.5	6.51 (d, 8.0 Hz)	117.7	6.51 (d, 8.2 Hz)/6.52 (d, 8.2 Hz)	117.2
14′	6.69 (dd, 8.1,1.9 Hz)	120.3	6.69 (dd, 8.1,2.0 Hz)	120.3	6.70 (dd, 8.0,2.0 Hz)	120.3	6.77 (dd, 8.2,1.9 Hz)/6.78 (dd, 8.2,1.9 Hz)	118.0
3′-OMe	3.66 (s)	54.8	3.66 (s)	54.8	3.66 (s)	54.8	3.63 (s) ×2	54.8
5′-OH	9.28 (s)	-	9.26 (s)	-	9.26 (s)	-	9.24 (s)	-
8′-OH							5.20 (d, 4.6 Hz) ×2	-
11′-OMe	3.75 (s)	55.6	3.75 (s)	55.6	3.73 (s)	55.5	3.74 (s) ×2	55.7

[a]×2 indicates two multiplets with almost identical chemical shifts.

8,8′-dihydroxy-12-*O*-12′,13−13′-bigigantol (**12**): NMR data see Table 2. HRESIMS m/z 561.2115 $[M + H]^+$ (calcd. $C_{32}H_{33}O_9$ for 561.2119, Δ = −0.71 ppm).

8,8′-dihydroxy-13-*O*-12′-bigigantol (**13**): NMR data see Table 3. HRESIMS m/z 577.2074 $[M - H]^-$ (calcd. $C_{32}H_{33}O_{10}$ for 577.2068, Δ = 1.04 ppm).

1−1′-biflavidin (**14**): ^{1}H NMR (DMSO-d_6, 600 MHz) δ 2.33 (2H, ddd, J = 15.1, 8.4, 6.2 Hz, H-10b), 2.43 (2H, ddd, J = 15.2, 8.8, 6.4 Hz, H-10a), 2.60 (4H, m, H_2-9), 5.01 (2H, d, J = 13.8 Hz, H-11b), 5.02 (2H, d, J = 13.8 Hz, H-11a), 6.32 (2H, s, H-3), 6.45 (2H, d, J = 2.2 Hz, H-6), 6.50 (2H, d, J = 2.2 Hz, H-8), 8.94 (2H, s, 2-OH), 9.31 (2H, s, 7-OH); ^{13}C NMR (DMSO-d_6, 151 MHz) δ 24.7 (CH_2-10), 27.2 (CH_2-9), 67.4 (CH_2-11), 100.8 (CH-3), 109.2 (CH-6), 111.1 (C-4a), 113.8 (CH-8), 116.0 (C-1), 118.4 (C-4b), 129.2 (C5), 133.4 (C-10a or C-8a), 134.2 (C-10a or C-8a), 151.5 (C-4), 155.1 (C-2), 156.1 (C-7). HRESIMS m/z 477.1333 $[M-H]^-$ (calcd for $C_{30}H_{21}O_6$, 477.1333, Δ = 0 ppm).

1−3′-biflavidin (**15**): ^{1}H NMR (DMSO-d_6, 600 MHz) δ 2.43 (2H, overlapped, H_2-10), 2.60 (2H, overlapped, H_2-9), 2.76 (4H, s, H_2-9′, H_2-10′), 4.85 (1H, d, J = 13.6 Hz, H-11′b), 4.89 (1H, d, J = 13.6 Hz, H-11′a), 5.00 (1H, d, J = 13.6 Hz, H-11b), 5.02 (1H, d, J = 13.6 Hz, H-11a), 6.29 (1H, s, H-3), 6.39 (1H, d, J = 2.3 Hz, H-6′), 6.39 (1H, s, H-1′), 6.45 (1H, d, J = 2.2 Hz, H-6), 6.50 (1H, d, J = 2.2 Hz, H-8), 6.55 (1H, d, J = 2.3 Hz, H-8′), 8.88 (1H, s, 2-OH), 8.91 (1H, s, 2′-OH), 9.30 (2H, s, 7′-OH, 7-OH); ^{1}C NMR (DMSO-d_6, 151 MHz) δ 25.0 (CH_2-10), 27.1 (CH_2-9), 27.2 (CH_2-9′), 27.3 (CH_2-10′), 67.3 (CH_2-11′), 67.5 (CH_2-11), 108.2 (CH-1′), 108.9 (CH-6′), 109.1 (CH-6), 109.9 (C-3′), 110.8 (C-4a), 111.1 (C-4a′), 113.6 (CH-8), 113.8 (CH-8′), 114.0 (C-1), 129.0 (C-5, C-5′), 133.3 (C-10a′, C-8a′), 133.5 (C-8a), 134.0 (C-10a), 150.8 (C-4′), 151.5 (C-4), 154.9 (C-2′), 155.3 (C-2), 156.0 (C-7), 156.1 (C-7′). HRESIMS m/z 477.1332 $[M - H]^-$ (calcd for $C_{30}H_{21}O_6$, 477.1333, Δ = −0.21 ppm).

https://doi.org/10.1021/acsomega.6c01880
ACS Omega XXXX, XXX, XXX−XXX

Table 4. NMR Spectroscopic Data (600 MHz, DMSO-d_6) for Compound 11

	compound **11**	
N°	δ_H (multiplicity,*J*)	δ_C
1	-	143.8, 144.1
2	6.14 (t, 2.2 Hz)	104.7
3	-	160.2
4	6.11 (t, 2.2 Hz)	98.8
5	-	158.2
6	6.16 (m)	107.9
7	2.53 (overlapped)	37.8
8	2.58 (overlapped)	36.9
9	-	130.7, 131.3
10	6.33 (d, 1.9 Hz)	105.8
11	-	147.8
12	-	133.1
13	-	146.7
14	5.95 (d, 1.9 Hz)	106.7
3-OMe	3.61 (s)	54.8
5-OH	9.22 (s)	-
11-OMe	3.65 (s)	55.8
1′	-	143.9
2′	6.29 (d, 2.3 Hz)	108.0
3′	-	160.3
4′	6.16 (m)	98.9
5′	-	158.4
6′	6.29 (d, 2.3 Hz)	105.0
7′	2.80 (m)	37.3
8′	2.85 (m)	37.1
9′	-	137.8
10′	6.95 (d, 2.1 Hz)	112.2
11′	-	151.8
12′	-	138.7
13′	-	124.4
14′	6.79 (d, 2.1 Hz)	123.5
3′-OMe	3.66 (s)	54.8
5′-OH	9.30 (s)	-
11′-OMe	3.66 (s)	55.8
1″	-	143.8 or 144.1
2″	6.16 (m)	104.8
3″	-	160.3
4″	6.13 (t, 2.2 Hz)	98.8
5″	-	158.3
6″	6.19 (t, 2.2 Hz)	107.9
7″	2.53 (overlapped)	37.6
8″	2.58 (overlapped)	36.9
9″	-	130.7 or 131.3
10″	6.68 (d, 2.0 Hz)	111.1
11″	-	147.3
12″	-	141.6
13″	-	132.9
14″	6.59 (d, 2.0 Hz)	122.4
3″-OMe	3.63 (s)	54.8
5″-OH	9.25 (s)	-
11″-OMe	3.74 (s)	55.7

Blestriarene A (**16**): ^{1}H NMR (DMSO-d_6, 600 MHz): δ 2.16 (2H, ddd, J = 14.6, 8.6, 4.9 Hz, H-9″), 2.25 (2H, ddd, J = 14.6, 9.2, 4.9 Hz, H-9′), 2.39 (2H, ddd, J = 13.5, 9.2, 4.9 Hz, H-10″), 2.45 (2H, ddd, J = 13.5, 8.6, 4.9 Hz, H-10′), 3.80 (6H, s, 5-OCH_3), 6.52 (2H, s, H-6), 6.55 (2H, d, J = 2.7 Hz, H-1), 6.59 (2H, dd, J = 8.7, 2.7 Hz, H-3), 7.93 (2H, d, J = 8.7 Hz, H-4), 8.89 (2H, s, 2-OH or 7-OH), 9.19 (2H, s, 2-OH or 7-OH); ^{13}C NMR (DMSO-d_6, 151 MHz) δ 26.8 (CH_2-9), 29.4 (CH_2-10), 55.2 (5-OCH_3), 97.9 (CH-6), 112.5 (CH-3), 113.9 (CH-1), 114.5 (C-4b), 115.2 (C-8), 124.4 (C-4a), 128.7 (CH-4), 138.7 (C-10a), 139.3 (C-8a), 154.3 (C-7), 154.9 (C-2), 155.9 (C-5). HRESIMS m/z 481.1649 $[M-H]^-$ (calcd for $C_{30}H_{25}O_6$, 481.1646, Δ = 0.62 ppm).

■ ASSOCIATED CONTENT

Supporting Information

The Supporting Information is available free of charge at https://pubs.acs.org/doi/10.1021/acsomega.6c01880.

Detailed experimental procedures for optimization of biotransformation conditions; NMR spectra (1H; COSY; 13C-DEPTQ; HSQC; HMBC; ROESY) of compounds **4**−**16** (DOCX)

■ AUTHOR INFORMATION

Corresponding Authors

Quentin Favre-Godal − *LVMH Recherche, Advanced Biobased & Bioinspired Ingredients Unit, St Jean de Braye 45800, France;* orcid.org/0000-0003-4950-515X; Phone: +33619585963; Email: qfavregodal@research.lvmh-pc.com

Katia Gindro − *Agroscope, Swiss Federal Research Station, Plant Protection, Mycology group, 1260 Nyon, Switzerland;* Phone: +41584604374; Email: katia.gindro@agroscope.admin.ch

Emerson Ferreira Queiroz − *School of Pharmaceutical Sciences, University of Geneva, CMU, Geneva 1211, Switzerland; Institute of Pharmaceutical Sciences of Western Switzerland, University of Geneva, CMU, Geneva 1211, Switzerland;* Phone: + 41223793641; Email: emerson.ferreira@unige.ch

Authors

Laurence Marcourt − *School of Pharmaceutical Sciences, University of Geneva, CMU, Geneva 1211, Switzerland; Institute of Pharmaceutical Sciences of Western Switzerland, University of Geneva, CMU, Geneva 1211, Switzerland;* orcid.org/0000-0002-9614-1099

Manon Giraud − *School of Pharmaceutical Sciences, University of Geneva, CMU, Geneva 1211, Switzerland; Institute of Pharmaceutical Sciences of Western Switzerland, University of Geneva, CMU, Geneva 1211, Switzerland*

Zeinab Karmime − *School of Pharmaceutical Sciences, University of Geneva, CMU, Geneva 1211, Switzerland; Institute of Pharmaceutical Sciences of Western Switzerland, University of Geneva, CMU, Geneva 1211, Switzerland*

Rémy Marcellin-Gros − *School of Pharmaceutical Sciences, University of Geneva, CMU, Geneva 1211, Switzerland; Institute of Pharmaceutical Sciences of Western Switzerland, University of Geneva, CMU, Geneva 1211, Switzerland;* orcid.org/0000-0002-5114-304X

Lorène Gourguillon − *LVMH Recherche, Advanced Biobased & Bioinspired Ingredients Unit, St Jean de Braye 45800, France;* orcid.org/0000-0002-4723-4088

Jean-Luc Wolfender − *School of Pharmaceutical Sciences, University of Geneva, CMU, Geneva 1211, Switzerland; Institute of Pharmaceutical Sciences of Western Switzerland, University of Geneva, CMU, Geneva 1211, Switzerland;* orcid.org/0000-0002-0125-952X

Complete contact information is available at: https://pubs.acs.org/10.1021/acsomega.6c01880

https://doi.org/10.1021/acsomega.6c01880
ACS Omega XXXX, XXX, XXX−XXX

Author Contributions

Conceptualization, Q.FG, K.G and E.F.Q; methodology, Q.FG, E.F.Q; formal analysis, Q.FG, M.G, R.MG, Z.K, L.M; investigation, Q.FG, M.G, Z.K, L.M, E.F.Q; data curation, Q.FG, R.MG, L.M; writing—original draft preparation, Q.FG, L.M and E.F.Q; writing—review and editing, Q.FG, L.M, L.G, K.G, J-L.W and E.F.Q; supervision, L.G, K.G and E.F.Q; project administration, L.G and J-L.W funding acquisition, L.G, J-L.W, K.G and E.F.Q.

Funding

This research was funded by Guerlain & LVMH Recherche to contribute to the understanding of orchids' phytochemistry and their preservation. The authors thank the Swiss National Science Foundation for providing financial support for this project, which aims to improve natural products chemical biodiversity for drug discovery by fungal secretome-assisted biotransformation (Grant N°205320_215078, EFQ, and KG).

Notes

The authors declare no competing financial interest.

■ ACKNOWLEDGMENTS

The authors thank Guerlain & LVMH Recherche as well as the Swiss National Science Foundation for providing financial support for this project. Some figures were created with BioRender.com icons, agreement number: XX29SR9B6M.

■ ABBREVIATIONS

1D, one-dimensional; 2D, two-dimensional; ABTS, 2,2′-azino-bis(3-ethylbenzothiazoline-6-sulfonic acid); BPI, base peak intensity; COSY, correlation spectroscopy; DMSO-d_6, deuterated dimethyl sulfoxide; ELSD, evaporative light scattering detector; ESI, electrospray ionization; EtOH, ethanol; H_2O, water; HBT, 1-hydroxybenzotriazole; HMBC, heteronuclear multiple bond correlation; HRMS, high resolution mass spectrometry; HSQC, heteronuclear single quantum coherence; MeOH, methanol; MS, mass spectrometry; NMR, nuclear magnetic resonance; PDA, photo diode array; UHPLC, ultra high-performance liquid chromatography

■ REFERENCES

(1) Schwarz, J.; Rosenthal, K.; Snajdrova, R.; Kittelmann, M.; Lütz, S. The Development of Biocatalysis as a Tool for Drug Discovery. *Chim. Int. J. Chem.* **2020**, *74* (5), 368−377.

(2) Palupi, K. D.; Oktavia, L.; Wulansari, D.; Fathoni, A.; Praptiwi, P.; Rahmi, D.; Agusta, A. Plant Endophytic Fungi: Powerful Catalytic Cells for Biotransformation of Chemical Structures of Biologically Active Compounds. *Chem. Biodivers.* **2025**, *22*, No. e202402281.

(3) Nagel, B.; Dellweg, H.; Gierasch, L. M. Glossary for Chemists of Terms Used in Biotechnology (IUPAC Recommendations 1992). *Pure Appl. Chem.* **1992**, *64* (1), 143−168.

(4) Schwartz, T. J.; O'Neill, B. J.; Shanks, B. H.; Dumesic, J. A. Bridging the Chemical and Biological Catalysis Gap: Challenges and Outlooks for Producing Sustainable Chemicals. *ACS Catal.* **2014**, *4* (6), 2060−2069.

(5) Choudhary, M.; Gupta, S.; Dhar, M. K.; Kaul, S. Endophytic Fungi-Mediated Biocatalysis and Biotransformations Paving the Way toward Green Chemistry. *Front. Bioeng. Biotechnol.* **2021**, *9*, 664705.

(6) Huber, R.; Marcourt, L.; Koval, A.; Schnee, S.; Righi, D.; Michellod, E.; Katanaev, V. L.; Wolfender, J.-L.; Gindro, K.; Queiroz, E. F. Chemoenzymatic Synthesis of Complex Phenylpropanoid Derivatives by the *Botrytis cinerea* Secretome and Evaluation of Their Wnt Inhibition Activity. *Front. Plant Sci.* **2022**, *12*, 805610.

(7) Gindro, K.; Schnee, S.; Righi, D.; Marcourt, L.; Nejad Ebrahimi, S.; Codina, J. M.; Voinesco, F.; Michellod, E.; Wolfender, J.-L.; Queiroz, E. F. Generation of Antifungal Stilbenes Using the Enzymatic Secretome of *Botrytis cinerea*. *J. Nat. Prod.* **2017**, *80* (4), 887−898.

(8) Huber, R.; Marcourt, L.; Héritier, M.; Luscher, A.; Guebey, L.; Schnee, S.; Michellod, E.; Guerrier, S.; Wolfender, J.-L.; Scapozza, L.; Köhler, T.; Gindro, K.; Queiroz, E. F. Generation of Potent Antibacterial Compounds through Enzymatic and Chemical Modifications of the Trans-δ-Viniferin Scaffold. *Sci. Rep.* **2023**, *13* (1), 15986.

(9) Huber, R.; Marcourt, L.; Quiros-Guerrero, L.-M.; Luscher, A.; Schnee, S.; Michellod, E.; Ducret, V.; Kohler, T.; Perron, K.; Wolfender, J.-L.; Gindro, K.; Ferreira Queiroz, E. Chiral Separation of Stilbene Dimers Generated by Biotransformation for Absolute Configuration Determination and Antibacterial Evaluation. *Front. Chem.* **2022**, *10*, 912396.

(10) Huber, R.; Koval, A.; Marcourt, L.; Héritier, M.; Schnee, S.; Michellod, E.; Scapozza, L.; Katanaev, V. L.; Wolfender, J.-L.; Gindro, K.; Ferreira Queiroz, E. Chemoenzymatic Synthesis of Original Stilbene Dimers Possessing Wnt Inhibition Activity in Triple-Negative Breast Cancer Cells Using the Enzymatic Secretome of *Botrytis cinerea* Pers. *Front. Chem.* **2022**, *10*, 881298.

(11) Huber, R.; Marcourt, L.; Félix, F.; Tardy, S.; Michellod, E.; Scapozza, L.; Wolfender, J.-L.; Gindro, K.; Queiroz, E. F. Study of Phenoxy Radical Couplings Using the Enzymatic Secretome of *Botrytis cinerea*. *Front. Chem.* **2024**, *12*, 1390066.

(12) Cardullo, N.; Muccilli, V.; Tringali, C. Laccase-Mediated Synthesis of Bioactive Natural Products and Their Analogues. *RSC Chem. Biol.* **2022**, *3* (6), 614−647.

(13) Martínez, A. T.; Ruiz-Dueñas, F. J.; Camarero, S.; Serrano, A.; Linde, D.; Lund, H.; Vind, J.; Tovborg, M.; Herold-Majumdar, O. M.; Hofrichter, M.; Liers, C.; Ullrich, R.; Scheibner, K.; Sannia, G.; Piscitelli, A.; Pezzella, C.; Sener, M. E.; Kılıç, S.; van Berkel, W. J. H.; Guallar, V.; Lucas, M. F.; Zuhse, R.; Ludwig, R.; Hollmann, F.; Fernández-Fueyo, E.; Record, E.; Faulds, C. B.; Tortajada, M.; Winckelmann, I.; Rasmussen, J.-A.; Gelo-Pujic, M.; Gutiérrez, A.; del Río, J. C.; Rencoret, J.; Alcalde, M. Oxidoreductases on Their Way to Industrial Biotransformations. *Biotechnol. Adv.* **2017**, *35* (6), 815−831.

(14) Agustin, M. B.; de Carvalho, D. M.; Lahtinen, M. H.; Hilden, K.; Lundell, T.; Mikkonen, K. S. Laccase as a Tool in Building Advanced Lignin-based Materials. *ChemSusChem* **2021**, *14* (21), 4615−4635.

(15) Janusz, G.; Pawlik, A.; Świderska-Burek, U.; Polak, J.; Sulej, J.; Jarosz-Wilkołazka, A.; Paszczyński, A. Laccase Properties, Physiological Functions, and Evolution. *Int. J. Mol. Sci.* **2020**, *21* (3), 966.

(16) Mayer, A. M.; Staples, R. C. Laccase: New Functions for an Old Enzyme. *Phytochemistry* **2002**, *60* (6), 551−565.

(17) Andersen, S. O. Insect Cuticular Sclerotization: A Review. *Insect Biochem. Mol. Biol.* **2010**, *40* (3), 166−178.

(18) Vinet, J.; Flourat, A. L.; Peyrot, C.; Brunois, F.; Brunissen, F.; Allais, F. Optimization and Green Metrics Analysis of the AgOAc-Mediated Dimerization of Piceid: Toward a High-Yielding and More Sustainable Access to δ-Viniferin and Synthesis of New Piceid Dimers. *ACS Sustain. Chem. Eng.* **2022**, *10* (28), 9166−9175.

(19) Sursin, E.; Flourat, A. L.; Akissi, Z. L. E.; Martinez, A.; Borie, N.; Peyrot, C.; Courot, E.; Nuzillard, J.-M.; Renault, J.-H.; Voutquenne-Nazabadioko, L.; Allais, F. Combining Laccase-Mediated Dimerization of Resveratrol and Centrifugal Partition Chromatography: Optimization of E-Labruscol Production and Identification of New Resveratrol Dimers. *ACS Sustain. Chem. Eng.* **2023**, *11* (31), 11559−11569.

(20) Mayolo-Deloisa, K.; González-González, M.; Rito-Palomares, M. Laccases in Food Industry: Bioprocessing, Potential Industrial and Biotechnological Applications. *Front. Bioeng. Biotechnol.* **2020**, *8*, 222.

(21) Kurniawati, S.; Nicell, J. A. Characterization of *Trametes versicolor* Laccase for the Transformation of Aqueous Phenol. *Bioresour. Technol.* **2008**, *99* (16), 7825−7834.

https://doi.org/10.1021/acsomega.6c01880
ACS Omega XXXX, XXX, XXX−XXX

(22) Eljounaidi, K.; Lichman, B. R. Nature's Chemists: The Discovery and Engineering of Phytochemical Biosynthesis. *Front. Chem.* **2020**, *8*, 596479.
(23) Akinwumi, B. C.; Bordun, K.-A. M.; Anderson, H. D. Biological Activities of Stilbenoids. *Int. J. Mol. Sci.* **2018**, *19* (3), 792.
(24) Koh, Y.-C.; Ho, C.-T.; Pan, M.-H. Recent Advances in Health Benefits of Stilbenoids. *J. Agric. Food Chem.* **2021**, *69* (35), 10036−10057.
(25) Zhou, X.-M.; Zheng, C.-J.; Chen, G.-Y.; Sun, C.-G.; Gan, L.-S.; Zhang, X.-P.; Song, X.-P.; Li, G.-N. Bioactive Phenanthrene and Bibenzyl Derivatives from the Stems of *Dendrobium nobile*. *J. Nat. Prod.* **2016**, *79* (7), 1791−1797.
(26) Natale, A. D.; Pollio, A.; Marco, A. D.; Luongo, G.; Fabio, G. D.; Zarrelli, A. Phenanthrene Dimers: Promising Source of Biologically Active Molecules. *Curr. Top. Med. Chem.* **2022**, *22* (11), 939−956.
(27) Vasas, A.; Merillon, J.-M.; Kodja, H. Phenanthrenes from Orchidaceae and Their Biological Activities. In *Orchids phytochemistry, biology and horticulture: fundamentals and applications*; Springer: Cham, 2022; pp 1−41.
(28) Keylor, M. H.; Matsuura, B. S.; Stephenson, C. R. J. Chemistry and Biology of Resveratrol-Derived Natural Products. *Chem. Rev.* **2015**, *115* (17), 8976−9027.
(29) John, S. E.; Tokala, R.; Kaki, V. R.; Shankaraiah, N. Expedition to Phenanthrene Nucleus: A Two-decade Research on Bench. *Asian J. Org. Chem.* **2021**, *10* (8), 2105−2136.
(30) Mamane, V.; Hannen, P.; Fürstner, A. Synthesis of Phenanthrenes and Polycyclic Heteroarenes by Transition-Metal Catalyzed Cycloisomerization Reactions. *Chem. Eur. J.* **2004**, *10* (18), 4556−4575.
(31) Xiao, K.; Zhang, H.-J.; Xuan, L.-J.; Zhang, J.; Xu, Y.-M.; Bai, D.-L. Stilbenoids: Chemistry and Bioactivities. *Stud. Nat. Prod. Chem.* **2008**, *34*, 453−646.
(32) Marti, G.; Schnee, S.; Andrey, Y.; Simoes-Pires, C.; Carrupt, P.-A.; Wolfender, J.-L.; Gindro, K. Study of Leaf Metabolome Modifications Induced by UV-C Radiations in Representative *Vitis, Cissus* and *Cannabis* Species by LC-MS Based Metabolomics and Antioxidant Assays. *Molecules* **2014**, *19* (9), 14004−14021.
(33) Schumpp, O.; Bruderhofer, N.; Monod, M.; Wolfender, J.-L.; Gindro, K. Ultraviolet Induction of Antifungal Activity in Plants. *Mycoses* **2012**, *55* (6), 507−513.
(34) Simmler, C.; Antheaume, C.; Lobstein, A. Antioxidant Biomarkers from *Vanda coerulea* Stems Reduce Irradiated HaCaT PGE-2 Production as a Result of COX-2 Inhibition. *PLoS One* **2010**, *5* (10), No. e13713.
(35) Simmler, C.; Lobstein, A.; Leplanquais, V.; André, P.; Archambault, J.; Bonté, F. In Vitro Anti-Inflammatory and Antioxidant Activities of Stilbenoids of *Vanda coerulea* (Orchidaceae). *Planta Med.* **2009**, *75*(09)..
(36) Pomini, A. M.; Sahyun, S. A.; Oliveira, S. M. D.; Faria, R. T. D. Bioactive Natural Products from Orchids Native to the Americas - A Review. *An. da Acad. Bras. Ciências* **2023**, *95* (suppl 1), No. e20211488.
(37) Chen, H.; Huang, Y.; Huang, J.; Lin, L.; Wei, G. Gigantol Attenuates the Proliferation of Human Liver Cancer HepG2 Cells through the PI3K/Akt/NF-κB Signaling Pathway. *Oncol. Rep.* **2017**, *37* (2), 865−870.
(38) Charoenrungruang, S.; Chanvorachote, P.; Sritularak, B.; Pongrakhananon, V. G. a Bibenzyl from *Dendrobium draconis*, Inhibits the Migratory Behavior of Non-Small Cell Lung Cancer Cells. *J. Nat. Prod.* **2014**, *77* (6), 1359−1366.
(39) Klongkumnuankarn, P.; Busaranon, K.; Chanvorachote, P.; Sritularak, B.; Jongbunprasert, V.; Likhitwitayawuid, K. Cytotoxic and Antimigratory Activities of Phenolic Compounds from *Dendrobium brymerianum*. *Évid.Based Complement. Altern. Med.* **2015**, *2015* (1), 1−9.
(40) Jayaprakasha, G. K.; Rao, L. J.; Sakariah, K. K. Antioxidant Activities of Flavidin in Different in Vitro Model Systems. *Bioorg. Med. Chem.* **2004**, *12* (19), 5141−5146.
(41) Majumder, P.; Laha, S.; Datta, N. Coelonin, A 9,10-Dihydrophenanthrene from the Orchids *Coelogyne ochracea* and *Coelogyne elata*. *Phytochemistry* **1982**, *21* (2), 478−480.
(42) Majumder, P. L.; Banerjee, S.; Maiti, D. C.; Sen, S. Stilbenoids from the Orchids *Agrostophyllum callosum* and *Coelogyne flaccida*. *Phytochemistry* **1995**, *39* (3), 649−653.
(43) Simmler, C. Etudes phytochimiques et biologiques de Vanda coerulea Griff ex. Lindl et de Vanda teres (Roxb) Lindl. (Orchidaceae); Ph.D. degree, 2010 https://www.theses.fr/2010STRA2065 (accessed 2022−07−25).
(44) Fu, X.; Chen, S.; Xian, S.; Wu, Q.; Shi, J.; Zhou, S. Dendrobium and Its Active Ingredients: Emerging Role in Liver Protection. *Biomed. Pharmacother.* **2023**, *157*, 114043.
(45) Kovács, A.; Vasas, A.; Hohmann, J. Natural Phenanthrenes and Their Biological Activity. *Phytochemistry* **2008**, *69* (5), 1084−1110.
(46) Bao, X.; Zu, Y.; Wang, B.; Li, M.; Jiang, F.; Qian, C.; Zhou, F.; Ding, Z. Coelonin Protects against PM2.5-induced Macrophage Damage via Suppressing TLR4/NF-κB/COX-2 Signaling Pathway and NLRP3 Inflammasome Activation in Vitro. *Environ. Toxicol.* **2023**, *38* (5), 1196−1210.
(47) Jiang, F.; Li, M.; Wang, H.; Ding, B.; Zhang, C.; Ding, Z.; Yu, X.; Lv, G. Coelonin, an Anti-Inflammation Active Component of *Bletilla striata* and Its Potential Mechanism. *Int. J. Mol. Sci.* **2019**, *20* (18), 4422.
(48) Al-Khayri, J. M.; Mascarenhas, R.; Harish, H. M.; Gowda, Y.; Lakshmaiah, V. V.; Nagella, P.; Al-Mssallem, M. Q.; Alessa, F. M.; Almaghasla, M. I.; Rezk, A. A.-S. Stilbenes, a Versatile Class of Natural Metabolites for Inflammation An Overview. *Molecules* **2023**, *28* (9), 3786.
(49) Righi, D.; Huber, R.; Koval, A.; Marcourt, L.; Schnee, S.; Le Floch, A.; Ducret, V.; Perozzo, R.; de Ruvo, C. C.; Lecoultre, N.; Michellod, E.; Ebrahimi, S. N.; Rivara-Minten, E.; Katanaev, V. L.; Perron, K.; Wolfender, J.-L.; Gindro, K.; Queiroz, E. F. Generation of Stilbene Antimicrobials against Multiresistant Strains of *Staphylococcus aureus* through Biotransformation by the Enzymatic Secretome of *Botrytis cinerea*. *J. Nat. Prod.* **2020**, *83* (8), 2347−2356.
(50) Liu, S.; Li, X.; Chen, B.; Ouyang, X.; Xie, Y.; Chen, D. Phytophenol Dimerization Reaction: From Basic Rules to Diastereoselectivity and Beyond. *Molecules* **2022**, *27* (15), 4842.
(51) Balcázar-López, E.; Méndez-Lorenzo, L. H.; Batista-García, R. A.; Esquivel-Naranjo, U.; Ayala, M.; Kumar, V. V.; Savary, O.; Cabana, H.; Herrera-Estrella, A.; Folch-Mallol, J. L. Xenobiotic Compounds Degradation by Heterologous Expression of a *Trametes sanguineus* Laccase in *Trichoderma atroviride*. *PLoS One* **2016**, *11* (2), No. e0147997.
(52) Han, M.-J.; Choi, H.-T.; Song, H.-G. Degradation of Phenanthrene by *Trametes versicolor* and Its Laccase. *J. Microbiol.* **2004**, *42* (2), 94−98.
(53) Guillarme, D.; Nguyen, D. T. T.; Rudaz, S.; Veuthey, J.-L. Method Transfer for Fast Liquid Chromatography in Pharmaceutical Analysis: Application to Short Columns Packed with Small Particle. Part II: Gradient Experiments. *Eur. J. Pharm. Biopharm.* **2008**, *68* (2), 430−440.
(54) Queiroz, E. F.; Guillarme, D.; Wolfender, J.-L. Advanced High-Resolution Chromatographic Strategies for Efficient Isolation of Natural Products from Complex Biological Matrices: From Metabolite Profiling to Pure Chemical Entities. *Phytochem. Rev.* **2024**, *23*, 1415−1442.
(55) Zhu, H.; Dai, O.; Zhou, F.; Yang, L.; Liu, F.; Liu, Y.; He, Y.-L.; Bu, L.; Guo, L.; Peng, C.; Xiong, L. Discovery of Bletillain, an Unusual Benzyl Polymer with Significant Autophagy-Inducing Effects in A549 Lung Cancer Cells through the Akt/GSK-3β/β-Catenin Signaling Pathway. *Bioorg. Chem.* **2021**, *117*, 105449.
(56) Shi, X.; Li, Y.; Liu, Y.; Jiang, J.; Wang, L.; Zhang, Y.; Chen, Y. A New 9,10-Dihydrophenanthropyran Dimer and a New Natural 9,10-Dihydrophenanthropyran from *Otochilus porrectus*. *Biochem. Syst. Ecol.* **2010**, *38* (4), 842−845.
(57) Yamaki, M.; Bai, L.; Inoue, K.; Takagi, S. Biphenanthrenes from *Bletilla striata*. *Phytochemistry* **1989**, *28* (12), 3503−3505.

https://doi.org/10.1021/acsomega.6c01880
ACS Omega XXXX, XXX, XXX−XXX

(58) Mehra, R.; Muschiol, J.; Meyer, A. S.; Kepp, K. P. A Structural-Chemical Explanation of Fungal Laccase Activity. *Sci. Rep.* **2018**, *8* (1), 17285.
(59) Queiroz, M. M. F.; Queiroz, E. F.; Zeraik, M. L.; Ebrahimi, S. N.; Marcourt, L.; Cuendet, M.; Castro-Gamboa, I.; Hamburger, M.; da Silva Bolzani, V.; Wolfender, J.-L. Chemical Composition of the Bark of *Tetrapterys mucronata* and Identification of Acetylcholinesterase Inhibitory Constituents. *J. Nat. Prod.* **2014**, *77* (3), 650−656.
(60) Reano, A. F.; Pion, F.; Domenek, S.; Ducrot, P.-H.; Allais, F. Chemo-Enzymatic Preparation and Characterization of Renewable Oligomers with Bisguaiacol Moieties: Promising Sustainable Anti-radical/Antioxidant Additives. *Green Chem.* **2016**, *18* (11), 3334−3345.
(61) Queiroz, E. F.; Alfattani, A.; Afzan, A.; Marcourt, L.; Guillarme, D.; Wolfender, J.-L. Utility of Dry Load Injection for an Efficient Natural Products Isolation at the Semi-Preparative Chromatographic Scale. *J. Chromatogr. A* **2019**, *1598*, 85−91.
(62) Quiros-Guerrero, L.-M.; Allard, P.-M.; Nothias, L.-F.; David, B.; Grondin, A.; Wolfender, J.-L. Comprehensive Mass Spectrometric Metabolomic Profiling of a Chemically Diverse Collection of Plants of the Celastraceae Family. *Sci. Data* **2024**, *11* (1), 415.

https://doi.org/10.1021/acsomega.6c01880
ACS Omega XXXX, XXX, XXX−XXX